Quantization of evanescent electromagnetic waves based on detector modes

Tetsuya Inoue
Department of Electronics, Yamanashi Industrial Technology College, 1308 Kamiozo, Enzan 404-0042, Japan

Hirokazu Hori
Department of Electronics, Yamanashi University, 4-3-11 Takeda, Kofu 400-8511, Japan
(Received 5 July 2000; published 9 May 2001)

The problem of field quantization in a half space is discussed based on the detector modes, which provide a useful basis for the study of atomic or molecular interaction with radiation modes involving evanescent electromagnetic waves. The detector modes, each of which involves a single outgoing wave, are introduced in terms of the time-reversal and spatial-rotation transforms of the widely used triplet modes given by Carniglia and Mandel. The derivation of the orthogonal relation for the detector modes is therefore straightforward. We represent the creation and annihilation operators for the detector modes in terms of those for the triplet modes, and obtain the field operator, Hamiltonian, number operator, and pseudomomentum operator. Based on this formalism, we evaluate the differential radiation probability for atomic dipole radiation near a dielectric surface. The evaluation of the final-state mode density is straightforward for the detector modes involving single outgoing waves. With respect to the image dipole picture, the quantum-to-classical correspondence is clear in the detector-mode formalism.

DOI: 10.1103/PhysRevA.63.063805 PACS number(s): 42.50.Ct, 42.50.Lc, 03.65.Ta

I. INTRODUCTION

Photon emission characteristics of atoms and molecules near a piece of matter have been studied extensively in relation to cavity quantum electrodynamics (cavity QED) [1–4] and optical near-field problems [5,6]. The important issues are the enhancement or reduction of spontaneous emission and the associated level shift of the radiating system due to variations of the environmental electromagnetic modes and to multiple interaction via the scattered electromagnetic field. Recently, these effects have been used to control the motion and radiative properties of atoms and molecules, especially by using high-Q optical resonators [7–10]. Cavity-QED phenomena in a broad sense also arise in near-field optical regimes, or in optical near-field interactions of a radiating system with matter lying in the vicinity of its subwavelength. Extensive studies have been made of the radiation properties of atoms and molecules near a material surface [11–13], and also of applications such as atom manipulation [14–16]. Further interest in the near-field regime lies in the photon emission characteristics of mesoscopic electronic systems, such as quantum dots and wires, fabricated on a substrate, and also in their observation by optical near-field microscopy and spectroscopy. One might expect several interesting effects to arise in the near-field regime which reflect the properties of the optical near field as an effective field or a coupled mode of the electromagnetic field with matter. That is, the dispersion relations and polarization properties of optical near fields deviate from those of photons in vacuum. Although optical near-field interactions, in general, have a relatively short period compared with those of high-Q cavities they still exert a considerable effect because of the high field intensity of the spatially localized fields. For further study in this direction, it is important to develop a quantum-mechanical treatment of the optical near field.

So far, theoretical studies have been reported of the photon emission and absorption properties of atoms and molecules near a planar material surface. The important issue involved in these half-space problems is the interaction with evanescent electromagnetic fields [12,17–19]. For example, when a homogeneous plane wave is incident at a planar dielectric boundary from the higher-refractive-index side with an angle beyond the critical angle of total internal reflection, an evanescent wave builds up in the lower-index side, propagating parallel to the boundary surface and exhibiting an exponential decay in the direction normal to the surface. This in turn suggests that, for an excited atom or molecule placed in the subwavelength vicinity of a dielectric surface (the optical near-field regime), the spontaneous radiation process involves both homogeneous and evanescent waves in the final state of the radiative quantum transition. The interaction with evanescent waves drives additional outgoing waves into the half space of the dielectric side with a transmission angle beyond the critical angle of total internal reflection [12,11]. This should result in a variation of the atomic radiative lifetime as a cavity-QED effect in the broad sense; the lifetime exhibits an exponential dependence on the atom-surface distance. Therefore, field quantization including evanescent waves has been extensively studied as the basis of general optical near-field problems. It is essential to study planar boundary problems since, as is shown in classical electromagnetic treatments, the scattered electromagnetic field from dielectrics of arbitrary shape can be described in terms of a set of homogeneous and evanescent waves by using the angular spectrum representation [20–22]. That is, if we understand the nature of atomic radiation near a planar dielectric surface, we can extend the results to cases of arbitrary-shaped dielectric boundaries by means of the angular spectrum representation of the scattered field [22].

The spontaneous decay rate of atomic excitation and the related angular distribution of radiation have been studied both experimentally and theoretically for atomic and molecu-

lar dipoles put near a planar dielectric surface [3,23–25]. In our previous work, we extended the theoretical study to the interaction of atomic multipoles with evanescent waves in the semiclassical regime based on analytical expressions for the radiation field using the angular spectrum representation of vector spherical waves [22]. Our numerical results for electric-dipole radiation with arbitrary orientation are in good agreement both with the numerical results reported by Lukosz [25] and with the experimental results reported by us obtained from the high-resolution laser spectroscopy of Cs atomic vapor near a dielectric surface at the D_2 resonance line [12,13]. Besides atomic and molecular cases, the similar effects might also be expected for quantum dots and wires lying on a substrate and also for their radiation measurements via optical near-field microscopy, although they have not yet been studied systematically [26].

According to Fermi's golden rule the probability of a quantum-mechanical transition depends on both the transition matrix element and the density of final states. The source of our interest in cavity-QED problems lies in the possibility of controlling the final-state density, especially for electromagnetic modes involved in the radiative transition under consideration. That is, the electromagnetic final state depends strongly on the scheme of our experiment. Therefore, in a practical analysis of experimental cavity-QED results, we should consider sources and sinks of photons as reservoirs being implemented outside the photonic system (i.e., far-field observation), each of which couples to one of the incident and outgoing wave components belonging to the photonic mode under consideration. In fact, we can consider several different situations of measurements in a quantum treatment, which determine the method of evaluating the final state of the corresponding transition event. In our context of a radiation study, these are classified roughly into two categories: single-photon-counting measurements and photon-correlation measurements. In the former only one of the photodetectors detects single photons, but in the latter signals from several pairs of photodetectors exhibit correlation features reflecting the coherence of the radiation. In any case, the quantum electrodynamic processes are evaluated in terms of external sources coupling to incident waves and external detectors coupling to outgoing waves, both being placed outside the isolated quantum system under consideration. Therefore, a careful consideration is also required of the role of sources and detectors for practical near-field optical measurements concerned with both excitation and interactions of the local mode or its observation in far field, so that the entire process considered here exhibits the nature of an open system. Depending on our experimental scheme, we can select a convenient set of basis functions to describe the electromagnetic mode. Here, it is noted that, for a study of the level shift of a radiative system, the important process lies rather in the closed system of multiple interactions between the radiative system and the electromagnetic field.

For the basis of field quantization including evanescent waves, Carniglia and Mandel introduced the so-called triplet modes [18]: the set of incident, reflected, and transmitted waves connected via Fresnel relations at the planar boundary under consideration. The triplet mode involving a single incident wave serves as a convenient basis for the theoretical treatment of photon absorption processes near a dielectric surface, where a single light source placed in far field may be assumed in a practical setup. On the other hand, when we study photon emission processes near a dielectric surface, we usually consider a practical setup with a photon-counting scheme by using an independent photodetector placed in each of the half spaces separated by the boundary, so that we may consider a single outgoing wave as the final state of the radiation process. This process is interpreted, in terms of the triplet-mode description, as a result of interference between the right and left triplet modes involving the outgoing wave under consideration. This situation, in some sense, is similar to beam-splitter problems. In this case, a much more convenient basis for the theoretical analysis is provided by the so-called detector-mode function including a single outgoing wave, especially when considering the radiative lifetime of atoms and molecules. Indeed, completeness of basis functions assures equivalence between various descriptions, but the practical treatment of photon absorption or emission experiments is simplified by choosing either of those expressions according to the experimental setup under consideration: either a single source or a single detector is assumed in the far-field region. The detector mode was introduced by Vigoureux and Payen in their theoretical study of the Raman diffusion due to atoms near a planar dielectric boundary [19]. In their work, the detector mode was defined in terms of a linear combination of the triplet-mode functions but was not explicitly quantized.

In the present work, we study the field quantization based on the detector modes as the basis for a theoretical analysis of photon emission process in the optical near field. This paper corresponds to the first part of a quantum-mechanical study of the radiation properties and radiative lifetime of oscillating electric and magnetic multipoles of arbitrary order near a planar dielectric surface based on a second-quantization formalism developed on the basis of the detector modes. In contrast to the study reported by Vigoureux and Payen [19], we introduce the detector modes in terms of time-reversal and spatial-rotation transforms of the triplet modes. This enables us to make a straightforward evaluation of the radiative decay rate in terms of the final-state density of photonic modes and provides a clear understanding of the meaning of detector modes as well as of the correspondence between classical and quantum descriptions of electric- and magnetic-multipole radiation of two-level systems in the near-field regime. In related work, a classical treatment of this problem for magnetic and electric dipoles in a half space has been reported by Lukosz and Kunz [23–25], in which the boundary-value problem is solved using a combination of single-component magnetic and electric Hertz vectors to provide the total light emission intensity per unit time using Poynting's theorem. A semiclassical evaluation has been given by Wylie and Sipe for electric-dipole radiation near a planar boundary based on general quantum-electrodynamic linear-response theory [4,27]. A full quantum treatment of electric-quadrupole radiation for a spherical dielectric boundary has been reported by Klimov and Letokhov [28]. How-

ever, to the authors' knowledge, no systematic study has been reported so far of the quantum-mechanical treatment of the radiation from higher-order multipoles near a material surface.

The contents of this paper are as follows. According to the investigation of the meaning and importance of detector modes in relation to the roles of sources and sinks in optical near-field problems, we present the schemes of half-space problems to be considered (Sec. II) and a brief review of the triplet-mode formalism (Appendix A). The definition of detector-mode functions and the second-quantization formulation including evanescent waves are presented in Secs. III–V. As an application and verification, several numerical results are presented for electric-dipole radiation near a dielectric surface in Secs. VI and VII. To account for the electric-dipole radiation, we have reported experimental results of the angular intensity distribution of radiation from excited Cs atoms near a planar dielectric surface by means of high-resolution laser spectroscopy at the D_2 line [12]. The results obtained in the present work [21] are in good agreement with those experiments. In a subsequent paper we will extend this work and report the numerical results for the angular distribution of radiation and associated spontaneous lifetime for higher-order electric and magnetic multipoles near a planar dielectric surface [29], in which the detector-mode functions are expanded in terms of vector spherical waves. This is reported briefly in this paper.

II. HALF-SPACE PROBLEM

We consider a space half of which is filled with a nonmagnetic, transparent, homogeneous, and isotropic dielectric medium of refractive index n (the left half space, $z<0$), and the other half is vacuum (the right half space, $z\geqslant 0$) (see Fig. 1). We will consider the electric field $\mathbf{E}(\mathbf{r},t)$ and its (positive-frequency) Fourier component $\mathbf{E}_{(+)}(\mathbf{r},t)=\mathbf{E}(\mathbf{r})\exp(-iKt)$. Here, K is the optical frequency under consideration with the light velocity taken as unity, $c=1$. The complex amplitude $\mathbf{E}(\mathbf{r})$ satisfies the Helmholtz equation

$$\nabla^2\mathbf{E}(\mathbf{r})+K^2n^2(\mathbf{r})\mathbf{E}(\mathbf{r})=\mathbf{0}, \tag{1}$$

with the refractive-index function defined as

$$n(\mathbf{r})=\begin{cases} n & \text{for} \quad z<0 \\ 1 & \text{for} \quad z\geqslant 0, \end{cases} \tag{2}$$

where n is assumed to be real. For later convenience, we will denote the wave vectors of incoming fields from the left of the boundary as $\mathbf{k}=(k_x,k_y,k_z)$, and those of outgoing fields to the right of the boundary as $\mathbf{K}^{(D)}=(K_x,K_y,-K_z)$, which satisfy the relations

$$k=nK, \tag{3}$$

$$K_x=k_x, \tag{4}$$

$$K_y=k_y, \tag{5}$$

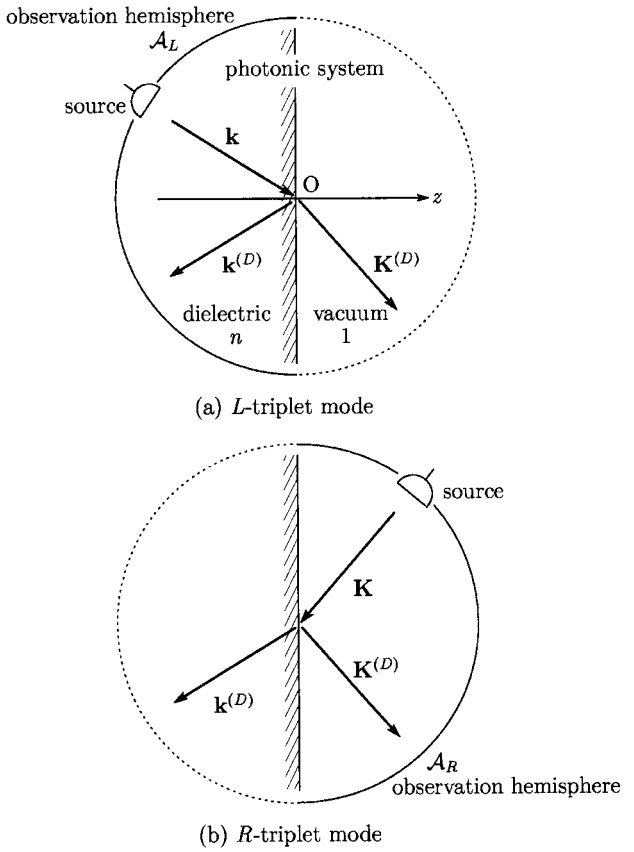

FIG. 1. The L and R triplet-mode configurations defined by Carniglia and Mandel [18]. The left half space $L(z<0)$ is filled with an isotropic medium of refractive index n and the right half space $L(z\geqslant 0)$ is vacuum. (a) L triplet-mode function. The incident-wave component is assumed to couple to a single source placed on the hemisphere $\mathcal{A}_L$ in far field. (b) R triplet mode with a single source placed on the hemisphere $\mathcal{A}_R$.

$$K_z=-\sqrt{(K^2-K_x^2-K_y^2)}, \tag{6}$$

$$k_z=+\sqrt{(k^2-k_x^2-k_y^2)}, \tag{7}$$

where K_z is negative in sign and k_z positive. $\mathbf{k}$ is always a real vector, but $\mathbf{K}^{(D)}$ becomes complex when $K_x^2+K_y^2>K^2$. We also denote the wave vectors of incoming fields from the right of the boundary as $\mathbf{K}=(K_x,K_y,K_z)$ and those of outgoing fields to the left of the boundary as $\mathbf{k}^{(D)}=(k_x,k_y,-k_z)$. In addition, let the projection of $\mathbf{k}$ and $\mathbf{K}$ onto the plane $z=0$ be $\mathbf{k}_\parallel=(k_x,k_y,0)$ and $\mathbf{K}_\parallel=(K_x,K_y,0)$, respectively. Here, $\mathbf{k}_\parallel=\mathbf{K}_\parallel=\mathbf{k}_\parallel^{(D)}=\mathbf{K}_\parallel^{(D)}$ due to phase continuity or the symmetry under parallel displacement with respect to the planar boundary. The triplet-mode description with these notations is presented in Appendix A.

Sources and sinks of light are introduced on the left $\mathcal{A}_L$ and the right $\mathcal{A}_R$ hemispheres of radius r_F lying in the far-field region, kr_F, $Kr_F\gg 1$, respectively. Each photonic source or detector interacts with the photonic system through coupling to one of the incoming and outgoing components of the triplet mode as shown in Figs. 1(a) and 1(b). When the absorption properties of atoms put into the photonic system

are considered in terms of one of the triplet modes, a single incident-wave component is coupled with a single source placed at far field, a point outside the photonic system under consideration. This corresponds to the illumination of atoms by a single photonic source. On the other hand, when the radiation properties of atoms are considered in terms of the triplet modes, we should take account of the phase relation between the right and left triplet modes of the corresponding wave vector in order to evaluate the correlation photon counts between two photodetectors, each of which is coupled with one of the outgoing-wave components of the triplet modes.

In contrast to the above, we can introduce the detector modes involving a single outgoing and two incident plane waves connected via the Fresnel relation at the boundary surface. In this scheme, when accounting for the absorption properties of atoms, two incident waves are considered to be coupled with a pair of correlated photonic sources. On the other hand, for radiation properties of atoms, the single outgoing-wave component of the detector mode is coupled with a single photonic detector. Therefore, the detector-mode description of photon emission processes can be related to a simple photon-counting measurement on either of the hemispheres $\mathcal{A}_L$ and $\mathcal{A}_R$.

III. DETECTOR-MODE FUNCTION

When we consider the far-field observation of spontaneous emission of atoms near a dielectric surface [see Figs. 2(a) and 2(b)], it is convenient to introduce the detector-mode functions coupled to a single light sink placed on either of the hemispheres $\mathcal{A}_L$ or $\mathcal{A}_R$. Here, we will define the detector-mode functions as the time reversal and spatial rotation of the triplet-mode functions. We will see that this provides us with a clear interpretation of the detector-mode description. It is noted that these transforms preserve the momentum parallel to the boundary surface as well as the angular momentum normal to the boundary surface, which represent the conserved quantities in the interacting atom plus photonic system under consideration. In the sense of restricted conservation laws, we refer to these quantities as pseudomomentum and pseudo-angular-momentum, respectively.

A. TC_2 transformation

Using the time reversal T and spatial rotation C_2 (see Appendix B), we can obtain the mode functions involving a single outgoing wave in either of the left and right half spaces with pseudomomentum $\hbar\mathbf{k}_\parallel$ for the TC_2 transform as follows.

$$\mathbf{E}_{(+)}(\mathbf{r},t)\rightarrow -[\mathbf{E}^{(D)}_{(+)}(-\mathbf{r}^{(D)},-t)]^*, \tag{8}$$

$$\mathbf{B}_{(+)}(\mathbf{r},t)\rightarrow [\mathbf{B}^{(D)}_{(+)}(-\mathbf{r}^{(D)},-t)]^*. \tag{9}$$

Here, the detector-mode vectors are labeled by the superscript (D), such as $\mathbf{v}^{(D)}=(v_x,v_y,-v_z)$, which corresponds to the triplet-mode vector $\mathbf{v}=(v_x,v_y,v_z)$. The subscript denotes the positive-frequency component of the field (see Appendix B).

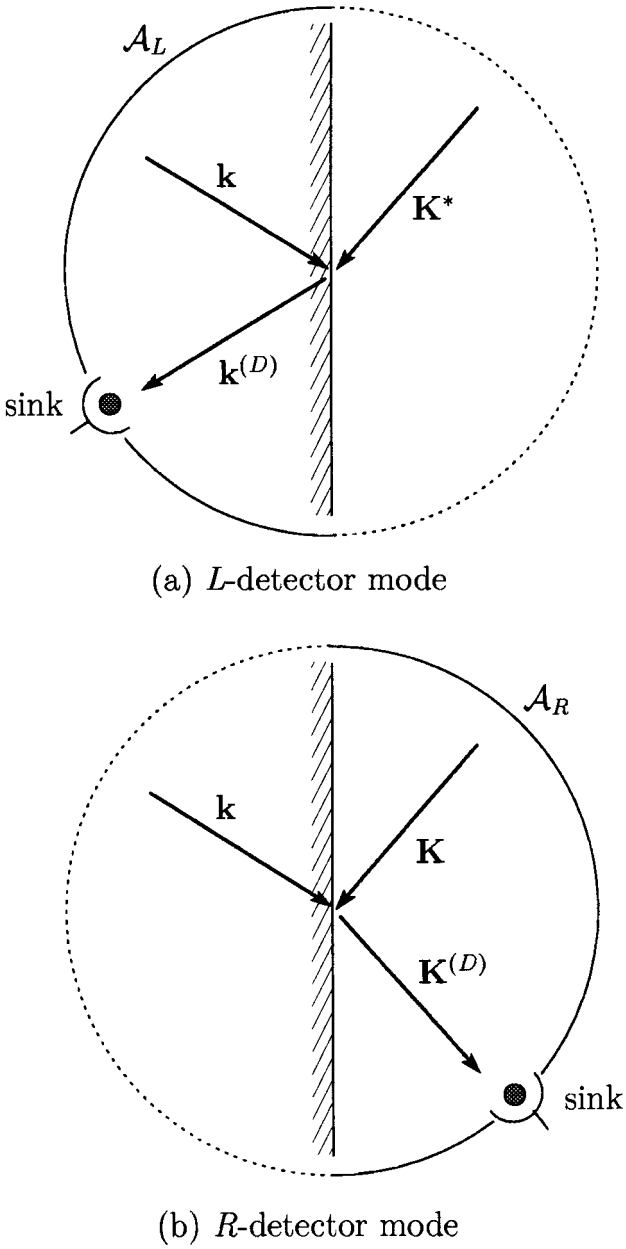

FIG. 2. The L and R detector-mode configurations. (a) L detector-mode function. The outgoing-wave component is assumed to couple to a single sink placed on the hemisphere $\mathcal{A}_L$ in far field. (b) R detector mode with a single sink placed on the hemisphere $\mathcal{A}_R$.

The transforms for wave vectors of L and R triplet mode functions (see Appendix A 1) are given, respectively, by

$$\mathbf{k}\rightarrow\mathbf{k}^{(D)},\quad \mathbf{k}^{(D)}\rightarrow\mathbf{k},\quad \mathbf{K}^{(D)}\rightarrow\mathbf{K}^*,$$

$$\mathbf{K}\rightarrow\mathbf{K}^{(D)},\quad \mathbf{K}^{(D)}\rightarrow\mathbf{K},\quad \mathbf{k}^{(D)}\rightarrow\mathbf{k}.$$

Under these transforms a single light source placed on the hemisphere $\mathcal{A}_L$ ($\mathcal{A}_R$) at a direction $-\mathbf{k}$ ($-\mathbf{K}$) from the origin

is transferred into a single light sink placed on $\mathcal{A}_L$ ($\mathcal{A}_R$) at the direction $\mathbf{k}^{(D)}$ ($\mathbf{K}^{(D)}$) (see Fig. 2). In addition, we will rewrite the Fourier components of the fields as $\eta\mathbf{E}_{(+)}(\mathbf{r},t)$ and $\eta\mathbf{B}_{(+)}(\mathbf{r},t)$ with $\eta=\pm 1$ for later convenience, according to the fact that electromagnetic fields in source-free space remain unchanged under such a replacement. Then we obtain the mode functions involving a single outgoing wave with pseudomomentum $\hbar\mathbf{k}_\parallel$ in either left or right half space for the transform $TC_2\eta$ as

$$\mathbf{E}_{(+)}(\mathbf{r},t)\rightarrow -\eta[\mathbf{E}^{(D)}_{(+)}(-\mathbf{r}^{(D)},-t)]^*, \tag{10}$$

$$\mathbf{B}_{(+)}(\mathbf{r},t)\rightarrow \eta[\mathbf{B}^{(D)}_{(+)}(-\mathbf{r}^{(D)},-t)]^*. \tag{11}$$

B. Detector-mode function

We will consider the behavior of the triplet-mode functions under the transform $TC_2\eta$. For example, the wave vectors and polarization vectors of each wave component of the L triplet modes are transformed as

$$(\mathbf{k},\boldsymbol{\varepsilon})\rightarrow(\mathbf{k}^{(D)},-\eta\boldsymbol{\varepsilon}),$$

$$(\mathbf{k}^{(D)},\boldsymbol{\varepsilon})\rightarrow(\mathbf{k},-\eta\boldsymbol{\varepsilon}),$$

$$(\mathbf{K}^{(D)},\boldsymbol{\varepsilon})\rightarrow(\mathbf{K}^*,-\eta\boldsymbol{\varepsilon}),$$

for TE ($\mu=1$), and as

$$(\mathbf{k},-(\boldsymbol{\kappa}\times\boldsymbol{\varepsilon}))\rightarrow(\mathbf{k}^{(D)},-\eta(\boldsymbol{\kappa}^{(D)}\times\boldsymbol{\varepsilon})),$$

$$(\mathbf{k}^{(D)},-(\boldsymbol{\kappa}^{(D)}\times\boldsymbol{\varepsilon}))\rightarrow(\mathbf{k},-\eta(\boldsymbol{\kappa}\times\boldsymbol{\varepsilon})),$$

$$(\mathbf{K}^{(D)},-(\mathbf{c}^{(D)}\times\boldsymbol{\varepsilon}))\rightarrow(\mathbf{K}^*,-\eta(\mathbf{c}^*\times\boldsymbol{\varepsilon})),$$

for TM ($\mu=2$). Then, choosing the factor $\eta=\eta_\mu$ as $\eta_1=-1$, $\eta_2=+1$, the detector-mode functions with a single outgoing wave are derived by the transform $TC_2\eta_\mu$ from the triplet-mode functions as follows:

$$\boldsymbol{\mathcal{E}}_{DL}(\mathbf{k}^{(D)},\mu,\mathbf{r})=-\eta_\mu[\boldsymbol{\mathcal{E}}^{(D)}_L(\mathbf{k},\mu,-\mathbf{r}^{(D)})]^*, \tag{12}$$

$$\boldsymbol{\mathcal{E}}_{DR}(\mathbf{K}^{(D)},\mu,\mathbf{r})=-\eta_\mu[\boldsymbol{\mathcal{E}}^{(D)}_R(\mathbf{K},\mu,-\mathbf{r}^{(D)})]^*, \tag{13}$$

$$\boldsymbol{\mathcal{B}}_{DL}(\mathbf{k}^{(D)},\mu,\mathbf{r})=\eta_\mu[\boldsymbol{\mathcal{B}}^{(D)}_L(\mathbf{k},\mu,-\mathbf{r}^{(D)})]^*, \tag{14}$$

$$\boldsymbol{\mathcal{B}}_{DR}(\mathbf{K}^{(D)},\mu,\mathbf{r})=\eta_\mu[\boldsymbol{\mathcal{B}}^{(D)}_R(\mathbf{K},\mu,-\mathbf{r}^{(D)})]^*. \tag{15}$$

Here, the suffix DL indicates that the mode involves outgoing waves into the medium (left to the boundary) with wave vector $\mathbf{k}^{(D)}$, and the suffix DR indicates those into vacuum (right to the boundary) with wave vector $\mathbf{K}^{(D)}$. Substituting Eq. (A1) into Eq. (12) and using Eqs. (A2)–(A7), the explicit form of the L detector-mode functions can be obtained [see Fig. 2(a)]. We can write down the results as

$$\boldsymbol{\mathcal{E}}_{DL}(\mathbf{k}^{(D)},\mu,\mathbf{r})=\boldsymbol{\mathcal{E}}^{(I)}_{DL}(\mathbf{k}^{(D)},\mu,\mathbf{r})+\boldsymbol{\mathcal{E}}^{(R)}_{DL}(\mathbf{k},\mu,\mathbf{r})+\boldsymbol{\mathcal{E}}^{(T)}_{DL}(\mathbf{K}^*,\mu,\mathbf{r}), \tag{16}$$

where

$$\boldsymbol{\mathcal{E}}^{(I)}_{DL}(\mathbf{k}^{(D)},1,\mathbf{r})=\begin{cases}\dfrac{1}{\sqrt{2}n}\boldsymbol{\varepsilon}\exp(i\mathbf{k}^{(D)}\cdot\mathbf{r}) & \text{for } z<0\\ \mathbf{0} & \text{for } z\geqslant 0,\end{cases} \tag{17}$$

$$\boldsymbol{\mathcal{E}}^{(R)}_{DL}(\mathbf{k},1,\mathbf{r})=\begin{cases}\dfrac{1}{\sqrt{2}n}\boldsymbol{\varepsilon}\dfrac{k_z+K_z^*}{k_z-K_z^*}\exp(i\mathbf{k}\cdot\mathbf{r}) & \text{for } z<0\\ \mathbf{0} & \text{for } z\geqslant 0,\end{cases} \tag{18}$$

$$\boldsymbol{\mathcal{E}}^{(T)}_{DL}(\mathbf{K}^*,1,\mathbf{r})=\begin{cases}\dfrac{1}{\sqrt{2}n}\boldsymbol{\varepsilon}\dfrac{2k_z}{k_z-K_z^*}\exp(i\mathbf{K}^*\cdot\mathbf{r}) & \text{for } z\geqslant 0\\ \mathbf{0} & \text{for } z<0,\end{cases} \tag{19}$$

$$\boldsymbol{\mathcal{E}}^{(I)}_{DL}(\mathbf{k}^{(D)},2,\mathbf{r})=\begin{cases}-\dfrac{1}{\sqrt{2}n}(\boldsymbol{\kappa}^{(D)}\times\boldsymbol{\varepsilon})\exp(i\mathbf{k}^{(D)}\cdot\mathbf{r}) & \text{for } z<0\\ \mathbf{0} & \text{for } z\geqslant 0,\end{cases} \tag{20}$$

$$\boldsymbol{\mathcal{E}}^{(R)}_{DL}(\mathbf{k},2,\mathbf{r})=\begin{cases}-\dfrac{1}{\sqrt{2}n}(\boldsymbol{\kappa}\times\boldsymbol{\varepsilon})\dfrac{k_z+n^2K_z^*}{k_z-n^2K_z^*}\exp(i\mathbf{k}\cdot\mathbf{r}) & \text{for } z<0\\ \mathbf{0} & \text{for } z\geqslant 0,\end{cases} \tag{21}$$

$$\boldsymbol{\mathcal{E}}^{(T)}_{DL}(\mathbf{K}^*,2,\mathbf{r})=\begin{cases}-\dfrac{1}{\sqrt{2}n}(\mathbf{c}^*\times\boldsymbol{\varepsilon})\dfrac{2nk_z}{k_z-n^2K_z^*}\exp(i\mathbf{K}^*\cdot\mathbf{r}) & \text{for } z\geqslant 0\\ \mathbf{0} & \text{for } z<0.\end{cases} \tag{22}$$

The magnetic field associated with the electric field $\boldsymbol{\mathcal{E}}_{DL}(\mathbf{k}^{(D)},\mu,\mathbf{r})$ is obtained immediately from Maxwell's equation as

$$\boldsymbol{\mathcal{B}}_{DL}(\mathbf{k}^{(D)},\mu,\mathbf{r})=\boldsymbol{\mathcal{B}}^{(I)}_{DL}(\mathbf{k}^{(D)},\mu,\mathbf{r})+\boldsymbol{\mathcal{B}}^{(R)}_{DL}(\mathbf{k},\mu,\mathbf{r})+\boldsymbol{\mathcal{B}}^{(T)}_{DL}(\mathbf{K}^*,\mu,\mathbf{r}). \tag{23}$$

In a similar way, substituting Eq. (A8) into Eq. (13) with the help of Eqs. (A9)–(A14), the explicit form of the R detector mode functions is obtained as follows [see Fig. 2(b)]:

$$\boldsymbol{\mathcal{E}}_{DR}(\mathbf{K}^{(D)},\mu,\mathbf{r})=\boldsymbol{\mathcal{E}}^{(I)}_{DR}(\mathbf{K}^{(D)},\mu,\mathbf{r})+\boldsymbol{\mathcal{E}}^{(R)}_{DR}(\mathbf{K},\mu,\mathbf{r})+\boldsymbol{\mathcal{E}}^{(T)}_{DR}(\mathbf{k},\mu,\mathbf{r}), \tag{24}$$

where

$$\boldsymbol{\mathcal{E}}_{DR}^{(I)}(\mathbf{K}^{(D)},1,\mathbf{r})=\begin{cases}\dfrac{1}{\sqrt{2}}\boldsymbol{\varepsilon}\exp(i\mathbf{K}^{(D)}\cdot\mathbf{r}) & \text{for } z\geqslant 0\\ \mathbf{0} & \text{for } z<0,\end{cases} \tag{25}$$

$$\boldsymbol{\mathcal{E}}_{DR}^{(R)}(\mathbf{K},1,\mathbf{r})=\begin{cases}\dfrac{1}{\sqrt{2}}\boldsymbol{\varepsilon}\dfrac{K_z+k_z}{K_z-k_z}\exp(i\mathbf{K}\cdot\mathbf{r}) & \text{for } z\geqslant 0\\ \mathbf{0} & \text{for } z<0,\end{cases} \tag{26}$$

$$\boldsymbol{\mathcal{E}}_{DR}^{(T)}(\mathbf{k},1,\mathbf{r})=\begin{cases}\dfrac{1}{\sqrt{2}}\boldsymbol{\varepsilon}\dfrac{2K_z}{K_z-k_z}\exp(i\mathbf{k}\cdot\mathbf{r}) & \text{for } z<0\\ \mathbf{0} & \text{for } z\geqslant 0,\end{cases} \tag{27}$$

$$\boldsymbol{\mathcal{E}}_{DR}^{(I)}(\mathbf{K}^{(D)},2,\mathbf{r})=\begin{cases}-\dfrac{1}{\sqrt{2}}(\mathbf{c}^{(D)}\times\boldsymbol{\varepsilon})\exp(i\mathbf{K}^{(D)}\cdot\mathbf{r}) & \text{for } z\geqslant 0\\ \mathbf{0} & \text{for } z<0,\end{cases} \tag{28}$$

$$\boldsymbol{\mathcal{E}}_{DR}^{(R)}(\mathbf{K},2,\mathbf{r})=\begin{cases}-\dfrac{1}{\sqrt{2}}(\mathbf{c}\times\boldsymbol{\varepsilon})\dfrac{n^2K_z+k_z}{n^2K_z-k_z}\exp(i\mathbf{K}\cdot\mathbf{r}) & \text{for } z\geqslant 0\\ \mathbf{0} & \text{for } z<0,\end{cases} \tag{29}$$

$$\boldsymbol{\mathcal{E}}_{DR}^{(T)}(\mathbf{k},2,\mathbf{r})=\begin{cases}-\dfrac{1}{\sqrt{2}}(\boldsymbol{\kappa}\times\boldsymbol{\varepsilon})\dfrac{2nK_z}{n^2K_z-k_z}\exp(i\mathbf{k}\cdot\mathbf{r}) & \text{for } z<0\\ \mathbf{0} & \text{for } z\geqslant 0.\end{cases} \tag{30}$$

The magnetic field associated with the electric field $\boldsymbol{\mathcal{E}}_{DR}(\mathbf{K}^{(D)},\mu,\mathbf{r})$ is given by Maxwell's equation as

$$\boldsymbol{\mathcal{B}}_{DR}(\mathbf{K}^{(D)},\mu,\mathbf{r})=\boldsymbol{\mathcal{B}}_{DR}^{(I)}(\mathbf{K}^{(D)},\mu,\mathbf{r})+\boldsymbol{\mathcal{B}}_{DR}^{(R)}(\mathbf{K},\mu,\mathbf{r})+\boldsymbol{\mathcal{B}}_{DR}^{(T)}(\mathbf{k},\mu,\mathbf{r}). \tag{31}$$

In a practical setup, $\mathbf{k}^{(D)}$ and $\mathbf{K}^{(D)}$, the outgoing wave vectors of the detector modes, correspond to the angular directions of the light sinks placed on $\mathcal{A}_L$ and $\mathcal{A}_R$, respectively. L and R detector modes correspond to the eigenstates of the pseudomomentum operator $-i\hbar\boldsymbol{\nabla}_{\parallel}$ as

$$(-i\hbar\boldsymbol{\nabla}_{\parallel})\boldsymbol{\mathcal{E}}_{DL}(\mathbf{k}^{(D)},\mu,\mathbf{r})=(\hbar\mathbf{k}_{\parallel})\boldsymbol{\mathcal{E}}_{DL}(\mathbf{k}^{(D)},\mu,\mathbf{r}), \tag{32}$$

$$(-i\hbar\boldsymbol{\nabla}_{\parallel})\boldsymbol{\mathcal{E}}_{DR}(\mathbf{K}^{(D)},\mu,\mathbf{r})=(\hbar\mathbf{k}_{\parallel})\boldsymbol{\mathcal{E}}_{DR}(\mathbf{K}^{(D)},\mu,\mathbf{r}), \tag{33}$$

where $-i\hbar\boldsymbol{\nabla}_{\parallel}$ operates on each component of $\boldsymbol{\mathcal{E}}$.

From the orthogonality relations for the triplet mode, Eqs. (A17)–(A19) in Appendix A with Eqs. (12) and (13), the orthogonality relations for the detector-mode functions are obtained as

$$\int[\boldsymbol{\mathcal{E}}_{DL}(\mathbf{k}^{(D)},\mu,\mathbf{r})]^*\cdot\boldsymbol{\mathcal{E}}_{DL}(\mathbf{k}'^{(D)},\mu',\mathbf{r})n^2(\mathbf{r})d^3x=\frac{1}{2}(2\pi)^3\delta_{\mu,\mu'}\delta^3(\mathbf{k}^{(D)}-\mathbf{k}'^{(D)}), \tag{34}$$

$$\int[\boldsymbol{\mathcal{E}}_{DR}(\mathbf{K}^{(D)},\mu,\mathbf{r})]^*\cdot\boldsymbol{\mathcal{E}}_{DR}(\mathbf{K}'^{(D)},\mu',\mathbf{r})n^2(\mathbf{r})d^3x=\frac{1}{2}(2\pi)^3\delta_{\mu,\mu'}\delta^3(\mathbf{K}^{(D)}-\mathbf{K}'^{(D)}), \tag{35}$$

$$\int[\boldsymbol{\mathcal{E}}_{DR}(\mathbf{K}^{(D)},\mu,\mathbf{r})]^*\cdot\boldsymbol{\mathcal{E}}_{DL}(\mathbf{k}'^{(D)},\mu',\mathbf{r})n^2(\mathbf{r})d^3x=0. \tag{36}$$

Here, the superscript (D) is put into the δ function because $\delta(x)=\delta(-x)$.

IV. TRANSFORMS BETWEEN TRIPLET MODES AND DETECTOR MODES

Since the $TC_2\eta$ transform of the triplet-mode functions can be described in terms of the superposition of the triplet-mode functions, $\boldsymbol{\mathcal{E}}_{DL}(\mathbf{k}^{(D)},\mu,\mathbf{r})$ and $\boldsymbol{\mathcal{E}}_{DR}(\mathbf{K}^{(D)},\mu,\mathbf{r})$ can be described as the superposition of $\boldsymbol{\mathcal{E}}_L(\mathbf{k},\mu,\mathbf{r})$ and $\boldsymbol{\mathcal{E}}_R(\mathbf{K},\mu,\mathbf{r})$,

$$\boldsymbol{\mathcal{E}}_{DL}(\mathbf{k}^{(D)},\mu,\mathbf{r})=(\mathcal{C}_{L,\mu}^{L})^*\boldsymbol{\mathcal{E}}_L(\mathbf{k},\mu,\mathbf{r})+\mathcal{C}_{L,\mu}^{R}\Theta_H\boldsymbol{\mathcal{E}}_R(\mathbf{K},\mu,\mathbf{r}), \tag{37}$$

$$\boldsymbol{\mathcal{E}}_{DR}(\mathbf{K}^{(D)},\mu,\mathbf{r})=\mathcal{C}_{R,\mu}^{L}\Theta_H\boldsymbol{\mathcal{E}}_L(\mathbf{k},\mu,\mathbf{r})+\mathcal{C}_{R,\mu}^{R}\Theta_H\boldsymbol{\mathcal{E}}_R(\mathbf{K},\mu,\mathbf{r}). \tag{38}$$

Here Θ_H is the projection function onto homogeneous modes defined by

$$\Theta_H=\Theta(\mathbf{k}_{\parallel}^2)-\Theta(\mathbf{k}_{\parallel}^2-\mathbf{K}^2), \tag{39}$$

where $\Theta(\mathbf{k}_{\parallel}^2)$ is the step function with respect to the argument $\mathbf{k}_{\parallel}^2=k_x^2+k_y^2$, so that $\Theta_H=1$ represents homogeneous waves and $\Theta_H=0$ evanescent waves. Equations (37) and (38) show that only the L detector modes involve evanescent waves, so long as the outgoing waves are propagating. The expansion coefficients $\mathcal{C}_{R,\mu}^{R}$, $\mathcal{C}_{R,\mu}^{L}$, $\mathcal{C}_{L,\mu}^{R}$, and $\mathcal{C}_{L,\mu}^{L}$ are derived using Eq. (A1) with the help of Eqs. (A2)–(A7), and Eq. (A8) with Eqs. (A9)–(A14), with the mode functions in Eqs. (16)–(22) and Eqs. (24)–(30), as

$$\mathcal{C}_{L,\mu}^{L}=\left(\frac{k_z+K_z}{k_z-K_z}\right)\delta_{\mu,1}+\left(\frac{k_z+n^2K_z}{k_z-n^2K_z}\right)\delta_{\mu,2}, \tag{40}$$

$$\mathcal{C}_{L,\mu}^{R}=\frac{1}{n}\left(\frac{2k_z}{k_z-K_z}\right)\delta_{\mu,1}+\frac{1}{n}\left(\frac{2nk_z}{k_z-n^2K_z}\right)\delta_{\mu,2}, \tag{41}$$

$$\mathcal{C}^L_{R,\mu} = n^2 \xi \mathcal{C}^R_{L,\mu}, \tag{42}$$

$$\mathcal{C}^R_{R,\mu} = -\mathcal{C}^R_{L,\mu}, \tag{43}$$

where the complex coefficient ξ is defined by

$$\xi = -\frac{K_z}{k_z}. \tag{44}$$

The following relations are also available:

$$(\mathcal{C}^L_{L,\mu})^* \mathcal{C}^L_{L,\mu} + n^2 \xi \mathcal{C}^R_{L,\mu} \mathcal{C}^R_{L,\mu} \Theta_H = 1, \tag{45}$$

$$(\mathcal{C}^L_{L,\mu})^* \mathcal{C}^R_{L,\mu} - \mathcal{C}^L_{L,\mu} \mathcal{C}^R_{L,\mu} \Theta_H = (\mathcal{C}^R_{L,\mu})^* (1 - \Theta_H). \tag{46}$$

Also, from Eqs. (37) and (38) with Eq. (45), we get the representations of the triplet-mode functions in terms of the detector-mode functions as follows:

$$\boldsymbol{\mathcal{E}}_L(\mathbf{k},\mu,\mathbf{r}) = \mathcal{C}^L_{L,\mu} \boldsymbol{\mathcal{E}}_{DL}(\mathbf{k}^{(D)},\mu,\mathbf{r}) + \mathcal{C}^R_{L,\mu} \Theta_H \boldsymbol{\mathcal{E}}_{DR}(\mathbf{K}^{(D)},\mu,\mathbf{r}), \tag{47}$$

$$\boldsymbol{\mathcal{E}}_R(\mathbf{K},\mu,\mathbf{r}) = \mathcal{C}^L_{R,\mu} \Theta_H \boldsymbol{\mathcal{E}}_{DL}(\mathbf{k}^{(D)},\mu,\mathbf{r}) + \mathcal{C}^R_{R,\mu} \Theta_H \boldsymbol{\mathcal{E}}_{DR}(\mathbf{K}^{(D)},\mu,\mathbf{r}). \tag{48}$$

V. FIELD QUANTIZATION BASED ON THE DETECTOR MODES

In the same manner as for the second-quantization formalism with the triplet modes, we can introduce the quantized electric-field operator based on the detector modes as

$$\begin{aligned}\hat{\mathbf{E}}(\mathbf{r},t) = {} & \frac{1}{(2\pi)^{3/2}} \int_{(-k_z)<0} d^3k^{(D)} \sum_{\mu=1}^{2} \left(\frac{\hbar K}{\epsilon}\right)^{1/2} \\ & \times [\hat{a}_{DL}(\mathbf{k}^{(D)},\mu) \boldsymbol{\mathcal{E}}_{DL}(\mathbf{k}^{(D)},\mu,\mathbf{r}) e^{-iKt} + \text{H.c.}] \\ & + \frac{1}{(2\pi)^{3/2}} \int_{(-K_z)>0} d^3K^{(D)} \sum_{\mu=1}^{2} \left(\frac{\hbar K}{\epsilon}\right)^{1/2} \\ & \times [\hat{a}_{DR}(\mathbf{K}^{(D)},\mu) \boldsymbol{\mathcal{E}}_{DR}(\mathbf{K}^{(D)},\mu,\mathbf{r}) e^{-iKt} + \text{H.c.}],\end{aligned} \tag{49}$$

where

$$\begin{aligned}\int_{(-k_z)<0} d^3k^{(D)} &= \int_{-\infty}^{\infty}\int_{-\infty}^{\infty}\int_{-\infty}^{0} dk_x dk_y d(-k_z) \\ &= \int_{k_z>0} d^3k,\end{aligned}$$

$$\begin{aligned}\int_{(-K_z)>0} d^3K^{(D)} &= \int_{-\infty}^{\infty}\int_{-\infty}^{\infty}\int_{0}^{\infty} dK_x dK_y d(-K_z) \\ &= \int_{K_z<0} d^3K.\end{aligned}$$

The operators $\hat{a}_{DL}(\mathbf{k}^{(D)},\mu)$, $\hat{a}^\dagger_{DL}(\mathbf{k}^{(D)},\mu)$ and also $\hat{a}_{DR}(\mathbf{K}^{(D)},\mu)$, $\hat{a}^\dagger_{DR}(\mathbf{K}^{(D)},\mu)$ indicate, respectively, the annihilation and creation operators of photons labeled by the polarization μ and the wave vectors $\mathbf{k}^{(D)}$ and $\mathbf{K}^{(D)}$ of outgoing waves to be coupled with photodetectors on either hemisphere $\mathcal{A}_L$ or $\mathcal{A}_R$ in the far field.

Here, we will investigate the commutation relations for the detector-mode operators. Since $\hat{a}_{DL}(\mathbf{k}^{(D)},\mu)$ and $\hat{a}_{DR}(\mathbf{K}^{(D)},\mu)$ can be described in terms of $\hat{a}_L(\mathbf{k},\mu)$ and $\hat{a}_R(\mathbf{K},\mu)$, we can utilize the commutation relations given for $\hat{a}_L(\mathbf{k},\mu)$ and $\hat{a}_R(\mathbf{K},\mu)$ by Eqs. (A21)–(A24). Substituting Eqs. (47) and (48) into Eq. (A20) with the help of Eqs. (45) and (46), and using the relations

$$\int_{k_z>0} d^3k\, \Theta_H = \int_{K_z<0} d^3K\, n^2 \xi \Theta_H, \tag{50}$$

$$\int_{K_z<0} d^3K\, \Theta_H = \int_{k_z>0} d^3k (n^2\xi)^{-1} \Theta_H \tag{51}$$

with $d^3k = -n^2 \xi\, d^3K$, we can obtain

$$\hat{a}_{DL}(\mathbf{k}^{(D)},\mu) = \mathcal{C}^L_{L,\mu} \hat{a}_L(\mathbf{k},\mu) + \mathcal{C}^R_{L,\mu} \Theta_H \hat{a}_R(\mathbf{K},\mu), \tag{52}$$

$$\hat{a}_{DR}(\mathbf{K}^{(D)},\mu) = \mathcal{C}^L_{R,\mu} \Theta_H \hat{a}_L(\mathbf{k},\mu) + \mathcal{C}^R_{R,\mu} \Theta_H \hat{a}_R(\mathbf{K},\mu). \tag{53}$$

The following relations hold for real variables:

$$\Theta_H \delta(\mathbf{K}-\mathbf{K}') = n^2 \xi \Theta_H \delta(\mathbf{k}-\mathbf{k}'), \tag{54}$$

$$\Theta_H \delta(\mathbf{k}-\mathbf{k}') = (n^2\xi)^{-1} \Theta_H \delta(\mathbf{K}-\mathbf{K}'). \tag{55}$$

For example, using Eqs. (45) and (54), we obtain

$$\begin{aligned}&[\hat{a}_{DL}(\mathbf{k}^{(D)},\mu), \hat{a}^\dagger_{DL}(\mathbf{k}'^{(D)},\mu')] \\ &\quad = \delta_{\mu,\mu'} [(\mathcal{C}^R_{L,\mu})^2 \Theta_H \delta(\mathbf{K}-\mathbf{K}') + (\mathcal{C}^L_{L,\mu})^* \mathcal{C}^L_{L,\mu} \delta(\mathbf{k}-\mathbf{k}')] \\ &\quad = \delta_{\mu,\mu'} [n^2 \xi (\mathcal{C}^R_{L,\mu})^2 \Theta_H + (\mathcal{C}^L_{L,\mu})^* \mathcal{C}^L_{L,\mu}] \delta(\mathbf{k}-\mathbf{k}') \\ &\quad = \delta_{\mu,\mu'} \delta(\mathbf{k}-\mathbf{k}') \\ &\quad = \delta_{\mu,\mu'} \delta(\mathbf{k}^{(D)} - \mathbf{k}'^{(D)}).\end{aligned}$$

Similarly, we have the whole set of commutation relations

$$[\hat{a}_{DL}(\mathbf{k}^{(D)},\mu), \hat{a}^\dagger_{DL}(\mathbf{k}'^{(D)},\mu')] = \delta_{\mu,\mu'} \delta(\mathbf{k}^{(D)} - \mathbf{k}'^{(D)}), \tag{56}$$

$$[\hat{a}_{DR}(\mathbf{K}^{(D)},\mu), \hat{a}^\dagger_{DR}(\mathbf{K}'^{(D)},\mu')] = \delta_{\mu,\mu'} \delta(\mathbf{K}^{(D)} - \mathbf{K}'^{(D)}), \tag{57}$$

with the trivial ones

$$[\hat{a}_{DL}(\mathbf{k}^{(D)},\mu), \hat{a}_{DR}(\mathbf{K}'^{(D)},\mu')] = 0, \tag{58}$$

$$[\hat{a}_{DL}(\mathbf{k}^{(D)},\mu), \hat{a}^\dagger_{DR}(\mathbf{K}'^{(D)},\mu')] = 0. \tag{59}$$

From Eqs. (52) and (53) with Eq. (45), the reversals of the relations in Eqs. (52) and (53) are given, respectively, by

$$\hat{a}_L(\mathbf{k},\mu) = (\mathcal{C}^L_{L,\mu})^* \hat{a}_{DL}(\mathbf{k}^{(D)},\mu) + \mathcal{C}^R_{L,\mu} \Theta_H \hat{a}_{DR}(\mathbf{K}^{(D)},\mu), \tag{60}$$

$$\hat{a}_R(\mathbf{K},\mu)=\mathcal{C}^L_{R,\mu}\Theta_H\hat{a}_{DL}(\mathbf{k}^{(D)},\mu)+\mathcal{C}^R_{R,\mu}\Theta_H\hat{a}_{DR}(\mathbf{K}^{(D)},\mu). \tag{61}$$

Finally, we consider the Hamiltonian $\hat{\mathcal{H}}$, number operator $\hat{\mathcal{N}}$, and pseudomomentum operator $\hat{\boldsymbol{\mathcal{P}}}_\parallel$ of the quantized electromagnetic fields. Substituting Eqs. (60) and (61) into Eqs. (A25)–(A27) and using Eqs. (45) and (46), we obtain

$$\hat{\mathcal{H}}=\int_{(-k_z)<0}d^3k^{(D)}\sum_{\mu=1}^{2}\hbar K\hat{a}^\dagger_{DL}(\mathbf{k}^{(D)},\mu)\hat{a}_{DL}(\mathbf{k}^{(D)},\mu)+\int_{(-K_z)>0}d^3K^{(D)}\sum_{\mu=1}^{2}\hbar K\hat{a}^\dagger_{DR}(\mathbf{K}^{(D)},\mu)\hat{a}_{DR}(\mathbf{K}^{(D)},\mu), \tag{62}$$

$$\hat{\mathcal{N}}=\int_{(-k_z)<0}d^3k^{(D)}\sum_{\mu=1}^{2}\hat{a}^\dagger_{DL}(\mathbf{k}^{(D)},\mu)\hat{a}_{DL}(\mathbf{k}^{(D)},\mu)+\int_{(-K_z)>0}d^3K^{(D)}\sum_{\mu=1}^{2}\hat{a}^\dagger_{DR}(\mathbf{K}^{(D)},\mu)\hat{a}_{DR}(\mathbf{K}^{(D)},\mu), \tag{63}$$

$$\hat{\boldsymbol{\mathcal{P}}}_\parallel=\int_{(-k_z)<0}d^3k^{(D)}\sum_{\mu=1}^{2}\hbar\mathbf{k}^{(D)}_\parallel\hat{a}^\dagger_{DL}(\mathbf{k}^{(D)},\mu)\hat{a}_{DL}(\mathbf{k}^{(D)},\mu)+\int_{(-K_z)>0}d^3K^{(D)}\sum_{\mu=1}^{2}\hbar\mathbf{k}^{(D)}_\parallel\hat{a}^\dagger_{DR}(\mathbf{K}^{(D)},\mu)\hat{a}_{DR}(\mathbf{K}^{(D)},\mu). \tag{64}$$

Here, we have used the relation $\mathbf{k}^{(D)}_\parallel=\mathbf{k}_\parallel$. Our definition of detector modes as the $TC_2\eta$ transform of the triplet modes, including both homogeneous and evanescent waves, provides a general and clear representation compared with those given by Vigoureux and Payen. The eigenstates of $\hat{\mathcal{H}}$, $\hat{\mathcal{N}}$, and $\hat{\boldsymbol{\mathcal{P}}}_\parallel$ are produced by operating $\hat{a}^\dagger_{DL}(\mathbf{k}^{(D)},\mu)$ and $\hat{a}^\dagger_{DR}(\mathbf{K}^{(D)},\mu)$ on the vacuum state $|0\rangle$. For example, the single-photon eigenstates with the energy eigenvalue $\hbar K$ are given by

$$|D,1(\mathbf{k}^{(D)},\mu)\rangle=\hat{a}^\dagger_{DL}(\mathbf{k}^{(D)},\mu)|0\rangle, \tag{65}$$

$$|D,1(\mathbf{K}^{(D)},\mu)\rangle=\hat{a}^\dagger_{DR}(\mathbf{K}^{(D)},\mu)|0\rangle, \tag{66}$$

where D indicates the states of the detector modes. The normalization relations are given by

$$\langle D,1(\mathbf{k}^{(D)},\mu)|D,1(\mathbf{k}'^{(D)},\mu')\rangle=\delta_{\mu,\mu'}\delta(\mathbf{k}^{(D)}-\mathbf{k}'^{(D)}), \tag{67}$$

$$\langle D,1(\mathbf{K}^{(D)},\mu)|D,1(\mathbf{K}'^{(D)},\mu')\rangle=\delta_{\mu,\mu'}\delta(\mathbf{K}^{(D)}-\mathbf{K}'^{(D)}), \tag{68}$$

$$\langle D,1(\mathbf{K}^{(D)},\mu)|D,1(\mathbf{k}'^{(D)},\mu')\rangle=0, \tag{69}$$

with $\langle 0|0\rangle=1$. From Eqs. (52) and (53), the states created by the detector-mode operators $\hat{a}^\dagger_{DL}(\mathbf{k}^{(D)},\mu),\hat{a}^\dagger_{DR}(\mathbf{K}^{(D)},\mu)$ can be described in terms of those created by the triplet-mode operators $\hat{a}^\dagger_L(\mathbf{k}^{(D)},\mu),\hat{a}^\dagger_R(\mathbf{K}^{(D)},\mu)$,

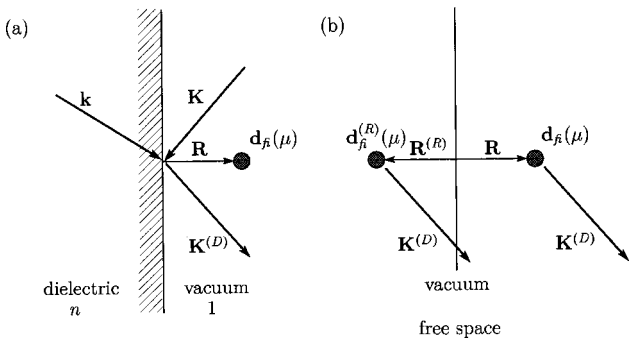

FIG. 3. The interaction of an atom with the R detector mode. The interaction between the atom and $\boldsymbol{\mathcal{E}}^{(R)}_{DR}$ component is equivalent to the radiation from an image dipole $\mathbf{d}^{(R)}_{fi}(\mu)$ placed at $\mathbf{R}^{(R)}$ in completely free space.

$$|D,1(\mathbf{k}^{(D)},\mu)\rangle=(\mathcal{C}^L_{L,\mu})^*|T,1(\mathbf{k},\mu)\rangle+\mathcal{C}^R_{L,\mu}\Theta_H|T,1(\mathbf{K},\mu)\rangle, \tag{70}$$

$$|D,1(\mathbf{K}^{(D)},\mu)\rangle=\mathcal{C}^L_{R,\mu}\Theta_H|T,1(\mathbf{k},\mu)\rangle+\mathcal{C}^R_{R,\mu}\Theta_H|T,1(\mathbf{K},\mu)\rangle. \tag{71}$$

The reversals of these expressions are given by

$$|T,1(\mathbf{k},\mu)\rangle=\mathcal{C}^L_{L,\mu}|D,1(\mathbf{k}^{(D)},\mu)\rangle+\mathcal{C}^R_{L,\mu}\Theta_H|D,1(\mathbf{k}^{(D)},\mu)\rangle, \tag{72}$$

$$|T,1(\mathbf{K},\mu)\rangle=\mathcal{C}^L_{R,\mu}\Theta_H|D,1(\mathbf{k}^{(D)},\mu)\rangle+\mathcal{C}^R_{R,\mu}\Theta_H|D,1(\mathbf{K}^{(D)},\mu)\rangle. \tag{73}$$

VI. RADIATION FROM AN ATOM NEAR A PLANAR DIELECTRIC BOUNDARY

Let us consider a photon emission process from an excited atom placed in the vacuum-side half space near a planar dielectric surface, as shown in Fig. 3(a). The interaction Hamiltonian is given by

$$\hat{V}(t)=-\frac{e}{m}\hat{\mathbf{A}}(\mathbf{r}_0+\mathbf{R},t)\cdot\mathbf{p}, \tag{74}$$

where $\mathbf{R}=(X,Y,Z)$ is the position vector of the atomic nucleus $(Z>0)$, $\mathbf{r}_0=(x_0,y_0,z_0)$ the relative position vector of the atomic electron with respect to the nucleus, and e, m, and $\mathbf{p}$ the electron charge, mass, and momentum, respectively. $\hat{\mathbf{A}}$ is the vector potential in the Coulomb gauge obtained from Eq. (49) by using the relation

$$\hat{\mathbf{E}}(\mathbf{r},t)=-(\partial/\partial t)\hat{\mathbf{A}}(\mathbf{r},t). \tag{75}$$

A. Radiation into the vacuum side

We will consider a photon emission process of a two-level atom with a μ-polarized outgoing wave in the vacuum-side half space with wave vector $\mathbf{K}^{(D)}=(K_x,K_y,-K_z)(-K_z>0)$. Here it is stressed that a single detector

mode is specified by its outgoing wave vector $\mathbf{K}^{(D)}$ and polarization μ. For photon emission into the detector mode specified by $\mathbf{K}^{(D)}$ and μ, the final state of the atom plus photon system is described by $|f\rangle = |D,1(\mathbf{K}^{(D)},\mu)\rangle|\varphi_f(\mathbf{r}_0,t)\rangle$, where $|\varphi_f\rangle$ corresponds to the atomic ground state. The initial state of the system is described by $|i\rangle = |0\rangle|\varphi_i(\mathbf{r}_0,t)\rangle$, with $|\varphi_i\rangle$ the atomic excited state under consideration. By separating the temporal evolution of the wave functions, the matrix element of the interaction Hamiltonian in Eq. (74) can be represented in terms of the time-independent matrix element V_{fi} as

$$V_{fi}(t) = V_{fi} e^{-i(\omega_0 - K)t}, \tag{76}$$

where ω_0 is the atomic transition frequency. The probability $d\Gamma$ of the $i \rightarrow f$ transition resulting in a single-photon emission is given by

$$d\Gamma = \frac{2\pi}{\hbar^2} |V_{fi}|^2 \delta(\omega_0 - K) d\rho(K), \tag{77}$$

where $d\rho(K)$ is the final-state mode density of the electromagnetic field.

When we consider single-photon emission into the vacuum side, the state of the photon is described by the R detector mode alone. From Eqs. (49) and (74), we can find the time-independent transition matrix element as

$$V_{fi}(\mathbf{K}^{(D)},\mu) = -i\frac{e}{m}\left[\frac{\hbar}{(2\pi)^3 K \epsilon}\right]^{1/2} \times \langle \varphi_f | [\boldsymbol{\mathcal{E}}_{DR}(\mathbf{K}^{(D)},\mu,\mathbf{r}_0+\mathbf{R})]^* \cdot \mathbf{p} | \varphi_i \rangle. \tag{78}$$

The atom in the vacuum side ($Z>0$) interacts with two components $\boldsymbol{\mathcal{E}}_{DR}^{(I)}$ and $\boldsymbol{\mathcal{E}}_{DR}^{(R)}$ of the R detector mode given in Eqs. (24)–(30). A single sink or photodetector is coupled with the outgoing wave of the R mode with the complex electric-field amplitude described by

$$\mathbf{E}_V(\mathbf{K}^{(D)},\mu,\mathbf{r}) = \begin{cases} \dfrac{E_0}{\sqrt{2}} \boldsymbol{\varepsilon} \exp(-i\mathbf{K}^{(D)} \cdot \mathbf{r}) & \text{for } \mu = 1 \\ \dfrac{E_0}{\sqrt{2}} (-\mathbf{c}^{(D)} \times \boldsymbol{\varepsilon}) \exp(-i\mathbf{K}^{(D)} \cdot \mathbf{r}) & \text{for } \mu = 2, \end{cases} \tag{79}$$

where

$$E_0 = \left[\frac{\hbar K}{(2\pi)^3 \epsilon_0}\right]^{1/2}. \tag{80}$$

Using the long-wavelength approximation and the relation $\langle \varphi_f | \mathbf{p} | \varphi_i \rangle = -im\omega_0 \langle \varphi_f | \mathbf{r}_0 | \varphi_i \rangle$, the matrix element can be written in the following form corresponding to the dipole approximation:

$$V_{fi}(\mathbf{K}^{(D)},\mu) = -(\omega_0/K)[\mathbf{d}_{fi}(\mu) \cdot \mathbf{E}_V(\mathbf{K}^{(D)},\mu,\mathbf{R}) + \mathbf{d}_{fi}^{(R)}(\mu) \cdot \mathbf{E}_V(\mathbf{K}^{(D)},\mu,\mathbf{R}^{(R)})]. \tag{81}$$

We consider the near-resonance condition and, hereafter, omit the factor (ω_0/K). The first term of Eq. (81) is attributed to radiation from a real electric dipole $\mathbf{d}_{fi}(\mu) = \langle \varphi_f | e\mathbf{r}_0 | \varphi_i \rangle$ placed at $\mathbf{R} = (X,Y,Z)$ with the electric field amplitude $\mathbf{E}_V$ entirely in free space [see Fig. 3(b)]. The second term can be interpreted as the radiation from an image dipole $\mathbf{d}_{fi}^{(R)}(\mu)$ placed at $\mathbf{R}^{(R)} = (X,Y,-Z)$ entirely in free space, so that $\mathbf{d}_{fi}^{(R)}(\mu)$ can be rewritten using the refractive index n of the medium as

$$\mathbf{d}_{fi}^{(R)}(\mu) = \begin{cases} \left(\dfrac{K_z + k_z}{K_z - k_z}\right) \langle \varphi_f | e\mathbf{r}_0 | \varphi_i \rangle & \text{for } \mu = 1 \\ \left(\dfrac{n^2 K_z + k_z}{n^2 K_z - k_z}\right) \langle \varphi_f | e\mathbf{r}_0^{(R)} | \varphi_i \rangle & \text{for } \mu = 2, \end{cases} \tag{82}$$

where $\mathbf{r}_0^{(R)} = (-x_0, -y_0, z_0)$.

The first term in the right-hand side of Eq. (81) represents the interaction of the atom with $\boldsymbol{\mathcal{E}}_{DR}^{(I)}$, so that $\boldsymbol{\mathcal{E}}_{DR}^{(I)}$ corresponds to the radiation field from the real dipole $\mathbf{d}_\mu$. The second term of Eq. (81) represents the interaction with $\boldsymbol{\mathcal{E}}_{DR}^{(R)}$, and $\boldsymbol{\mathcal{E}}_{DR}^{(R)}$ can be considered as the radiation field from the imaginary dipole which is often used in semiclassical treatments. The radiation field involves only one outgoing wave with wave vector $\mathbf{K}^{(D)}$ and polarization μ, so that the mode density $d\rho(K)$ for the final state of the photon for each μ is given simply by

$$d\rho(K) = d^3\mathbf{K}^{(D)} = K^2 dK\, d\Omega(\mathbf{c}^{(D)}), \tag{83}$$

with the infinitesimal solid angle $d\Omega(\mathbf{c}^{(D)})$ in the direction of the unit propagation vector $\mathbf{c}^{(D)}$. Here, it is stressed that the detector mode provides a clear understanding of the radiation process from the viewpoints of the classical-quantum correspondence and the straightforward evaluation of the final-state mode density discussed above. Such a straightforward interpretation is not available in the usual triplet-mode-based field quantization.

Substituting Eqs. (81) and (83) into Eq. (77) and integrating over dK, the differential radiation probability $d\Gamma$ for photon emission into the mode involving the outgoing wave with $\mathbf{K}^{(D)}$ lying in the solid angle $d\Omega(\mathbf{c}^{(D)})$ is given by

$$d\Gamma(\mathbf{c}^{(D)},\mu) = \left(\frac{2\pi K^2}{\hbar^2}\right) |\mathbf{d}_{fi}(\mu) \cdot \mathbf{E}_V(\mathbf{K}^{(D)},\mu,\mathbf{R}) + \mathbf{d}_{fi}^{(R)}(\mu) \cdot \mathbf{E}_V(\mathbf{K}^{(D)},\mu,\mathbf{R}^{(R)})|^2 d\Omega(\mathbf{c}^{(D)}), \tag{84}$$

where $K = \omega_0$.

B. Radiation into the medium side

Next, we will consider emission of a μ-polarized photon resulting in an outgoing wave in the medium side with $\mathbf{k}^{(D)}$

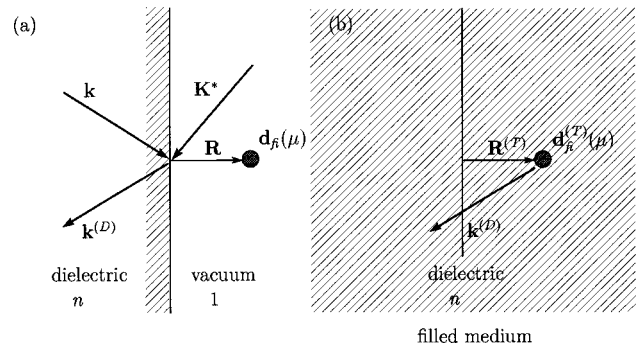

FIG. 4. The interaction of an atom with the L detector mode. The interaction between the atom and $\boldsymbol{\mathcal{E}}_{DL}^{(L)}$ component is equivalent to the radiation from a dipole $\mathbf{d}_{fi}^{(T)}(\mu)$ placed at $\mathbf{R}^{(T)}$ in a space entirely filled with dielectric medium.

$=(k_x,k_y,-k_z)(-k_z<0)$. The final state corresponds to $|f\rangle=|D,1(\mathbf{k}^{(D)},\mu)\rangle|\varphi_f\rangle$. From Eqs. (49) and (74), the time-independent matrix element of the interaction Hamiltonian is given by

$$V_{fi}(\mathbf{k}^{(D)},\mu)=-i\frac{e}{m}\left[\frac{\hbar}{(2\pi)^3K\epsilon}\right]^{1/2}\times\langle\varphi_f|[\boldsymbol{\mathcal{E}}_{DL}(\mathbf{k}^{(D)},\mu,\mathbf{r}_0+\mathbf{R})]^*\cdot\mathbf{p}|\varphi_i\rangle. \tag{85}$$

According to Eqs. (16)–(22), the atom interacts with the field only via the $\boldsymbol{\mathcal{E}}_{DL}^{(T)}$ component of the L detector mode. The transition matrix element can be written as

$$V_{fi}(\mathbf{k}^{(D)},\mu)=-(\omega_0/K)\mathbf{d}_{fi}^{(T)}(\mu)\cdot\mathbf{E}_M(\mathbf{k}^{(D)},\mu,\mathbf{R}^{(T)}), \tag{86}$$

with the electric-field amplitude of the outgoing wave

$$\mathbf{E}_M(\mathbf{k}^{(D)},\mu,\mathbf{r})=\begin{cases}\dfrac{E_0}{\sqrt{2}n}\boldsymbol{\varepsilon}\exp(-i\mathbf{k}^{(D)}\cdot\mathbf{r}) & \text{for } \mu=1\\ \dfrac{E_0}{\sqrt{2}n}(-\boldsymbol{\kappa}^{(D)}\times\boldsymbol{\varepsilon})\exp(-i\mathbf{k}^{(D)}\cdot\mathbf{r}) & \text{for } \mu=2.\end{cases} \tag{87}$$

This shows that the radiation process, viewed from the medium-side half space, is equivalent to that from an electric dipole $\mathbf{d}_{fi}^{(T)}(\mu)=\langle\varphi_f|\mathbf{d}^{(T)}(\mu)|\varphi_i\rangle$ placed at $\mathbf{R}^{(T)}=(X,Y,\xi Z)$ in the entirely filled medium (see Fig. 4). Here the equivalent dipole moment operator $\mathbf{d}_{fi}^{(T)}(\mu)$ is described in terms of the transmission coefficient

$$\mathbf{d}_{fi}^{(T)}(\mu)=\begin{cases}\dfrac{1}{\xi}\left(\dfrac{2K_z}{K_z-k_z}\right)\langle\varphi_f|e\mathbf{r}_0|\varphi_i\rangle & \text{for } \mu=1\\ \dfrac{1}{\xi}\left(\dfrac{2nK_z}{n^2K_z-k_z}\right)\langle\varphi_f|e\mathbf{r}_0^{(T)}|\varphi_i\rangle & \text{for } \mu=2,\end{cases} \tag{88}$$

where $\mathbf{r}_0^{(T)}=n(\xi x_0,\xi y_0,z_0)$. It is noted that, since Eq. (86) represents the radiation via $\boldsymbol{\mathcal{E}}_{DL}^{(T)}$, the electric dipole $\mathbf{d}_{fi}^{(T)}(\mu)$ and its position $\mathbf{R}^{(T)}$ become complex vectors when the atom interacts with the evanescent wave in the L detector mode. As the final-state mode function is labeled by $\mathbf{k}^{(D)}$ and μ in $\boldsymbol{\mathcal{E}}_{DL}(\mathbf{k}^{(D)},\mu,\mathbf{r})$, the differential mode density $d\rho(K)$ is given simply by

$$d\rho(K)=d^3\mathbf{k}^{(D)}=n^3K^2dK\,d\Omega(\boldsymbol{\kappa}^{(D)}), \tag{89}$$

with the infinitesimal solid angle $d\Omega(\boldsymbol{\kappa}^{(D)})$ in the direction of the unit propagation vector $\boldsymbol{\kappa}^{(D)}$. Substituting Eqs. (86) and (89) into Eq. (77) and integrating over dK, the differential transition probability $d\Gamma$ is given by

$$d\Gamma(\boldsymbol{\kappa}^{(D)},\mu)=\left(\frac{2\pi n^3K^2}{\hbar^2}\right)\times|\mathbf{d}_{fi}^{(T)}(\mu)\cdot\mathbf{E}_M(\mathbf{k}^{(D)},\mu,\mathbf{R}^{(T)})|^2d\Omega(\boldsymbol{\kappa}^{(D)}). \tag{90}$$

VII. NUMERICAL EVALUATION OF THE ANGULAR DISTRIBUTION OF RADIATION INTO THE MEDIUM SIDE

As an example of numerical evaluation, we will consider the electric-dipole radiation near a planar dielectric surface. The atomic initial state is assumed to be an excited state without spin and described in terms of the superposition of states with orbital angular momentum $l=1$ oriented in the direction angle (Θ,Φ) by

$$|\varphi_i\rangle=\sum_m(-1)^mC_{-m}|\varphi_{\nu,1,m}\rangle, \tag{91}$$

where

$$C_{+1}=-\frac{1}{\sqrt{2}}\sin\Theta e^{i\Phi},\qquad C_0=\cos\Theta,\qquad C_{-1}=+\frac{1}{\sqrt{2}}\sin\Theta e^{-i\Phi}. \tag{92}$$

The ground state, or the final state of the atomic transition, is $|\varphi_f\rangle=|\varphi_{\nu',0,0}\rangle$.

Let us introduce the electric-dipole operators defined by

$$d_{+1}^{(1)}=-\frac{e}{\sqrt{2}}(x_0+iy_0),\qquad d_0^{(1)}=ez_0,\qquad d_{-1}^{(1)}=+\frac{e}{\sqrt{2}}(x_0-iy_0). \tag{93}$$

According to the Wigner-Eckart theorem, the matrix element of the electric-dipole operators is written by

$$\langle \varphi_{\nu',0,0}|d_m^{(1)}|\varphi_{\nu,1,m'}\rangle=(-1)^{1-m}\delta_{m',-m}\frac{\langle \varphi_{\nu',0}\|d^{(1)}\|\varphi_{\nu,1}\rangle}{\sqrt{3}}, \tag{94}$$

where $\langle \varphi_{\nu',0}\|d^{(1)}\|\varphi_{\nu,1}\rangle$ is the reduced matrix element. Thus we have the matrix elements of the electric dipole $\mathbf{d}_{fi}^{(T)}(\mu)$;

$$\mathbf{d}_{fi}^{(T)}(1)=-\frac{1}{\xi}\left(\frac{2K_z}{K_z-k_z}\right)\frac{\langle \varphi_{\nu',0}\|d^{(1)}\|\varphi_{\nu,1}\rangle}{\sqrt{3}} \times(\sin\Theta\cos\Phi,\sin\Theta\sin\Phi,\cos\Theta), \tag{95}$$

$$\mathbf{d}_{fi}^{(T)}(2)=-\frac{1}{\xi}\left(\frac{2nK_z}{n^2K_z-k_z}\right)\frac{\langle \varphi_{\nu',0}\|d^{(1)}\|\varphi_{\nu,1}\rangle}{\sqrt{3}} \times n(\xi\sin\Theta\cos\Phi,\xi\sin\Theta\sin\Phi,\cos\Theta). \tag{96}$$

As in our previous work [21], we introduce spherical angles α_1, α_2, and β as shown in Fig. 5 for the L detector mode function. The vectors $\boldsymbol{\kappa}^{(D)}$ and $\boldsymbol{\varepsilon}$ are represented by

$$\boldsymbol{\kappa}^{(D)}=(\sin\alpha_2\cos\beta,\sin\alpha_2\sin\beta,-\cos\alpha_2),$$

$$\boldsymbol{\varepsilon}=(-\sin\beta,\cos\beta,0),$$

$$\boldsymbol{\kappa}^{(D)}\times\boldsymbol{\varepsilon}=(\cos\alpha_2\cos\beta,\cos\alpha_2\sin\beta,\sin\alpha_2),$$

and $K_z=-K\cos\alpha_1$ and $k_z=nK\cos\alpha_2$. Here, α_1 is real ($0\leqslant\alpha_1<\pi/2$) for $0\leqslant\alpha_2<\alpha_{2c}=\arcsin(1/n)$. α_1 is complex for $\alpha_{2c}\leqslant\alpha_2<\pi/2$ and is described as $\alpha_1=(\pi/2)-i\gamma_1$ ($0\leqslant\gamma_1<\gamma_{1c}$), with $\sin[(\pi/2)-i\gamma_{1c}]=n$. α_{2c} is the critical angle of the total internal reflection. $(\pi/2)-i\gamma_{1c}$ is another critical angle corresponding to $\alpha_2=(\pi/2)$, above which waves in the dielectric side also become evanescent waves, so that the field forms a kind of localized mode on the boundary surface [21]. The differential transition probabilities in Eq. (90) are evaluated as

$$d\Gamma(\boldsymbol{\kappa}^{(D)},1)=\left(\frac{3n^3}{2\pi}\right)\Gamma_0\left|\frac{\cos\alpha_2\sin\Theta\sin(\beta-\Phi)}{\cos\alpha_1+n\cos\alpha_2}e^{iKZ\cos\alpha_1}\right|^2 d\Omega(\boldsymbol{\kappa}^{(D)}), \tag{97}$$

$$d\Gamma(\boldsymbol{\kappa}^{(D)},2)=\left(\frac{3n^3}{2\pi}\right)\Gamma_0\left|\frac{\cos\alpha_2[\cos\Theta\sin\alpha_1+\sin\Theta\cos(\beta-\Phi)\cos\alpha_1]}{n\cos\alpha_1+\cos\alpha_2}e^{iKZ\cos\alpha_1}\right|^2 d\Omega(\boldsymbol{\kappa}^{(D)}), \tag{98}$$

with the coefficient Γ_0 defined by

$$\Gamma_0=\frac{1}{4\pi\epsilon\hbar}\left(\frac{4K^3}{3}\right)\frac{|\langle \varphi_{\nu',0}\|d^{(1)}\|\varphi_{\nu,1}\rangle|^2}{3}. \tag{99}$$

This corresponds to the spontaneous emission rate in free space ($n\rightarrow1$). In practice, integration of the differential radiation probability over the left half space for $n\rightarrow1$ gives $\Gamma_0/2$:

$$\Gamma_0/2=\lim_{n\rightarrow1}\sum_{\mu}\int_{\mathcal{A}_L}d\Gamma(\boldsymbol{\kappa}^{(D)},\mu)\quad[(\Theta,\Phi)\rightarrow(0,0)]. \tag{100}$$

Figure 6 shows one of the numerical results of

$$d\Gamma(\boldsymbol{\kappa}^{(D)})/\Gamma_0=\sum_{\mu}d\Gamma(\boldsymbol{\kappa}^{(D)},\mu)/\Gamma_0, \tag{101}$$

calculated for $n=\sqrt{2}[\alpha_{2c}=(\pi/4)]$, $\rho=1$, and $\beta_1=0$ (zx plane). Since the angular intensity distribution $dI(\boldsymbol{\kappa}^{(D)},\mu)$ into the solid angle $d\Omega(\boldsymbol{\kappa}^{(D)})$ is given by $dI(\boldsymbol{\kappa}^{(D)},\mu)=\hbar Kd\Gamma(\boldsymbol{\kappa}^{(D)},\mu)$, the normalized probability of photon emission $d\Gamma(\boldsymbol{\kappa}^{(D)},\mu)/\Gamma_0$ equals the normalized intensity $dI(\boldsymbol{\kappa}^{(D)},\mu)/I_0$, with total radiation intensity I_0. Our present results are in agreement with those obtained by a classical treatment in our previous work [21] based on the angular spectrum representation of electromagnetic fields, for which a comparison with experimental results [12] has also been reported. As the experimental results given in Ref. [12] are for the optical transition between the hyperfine states of Cs atoms at the D_2 line ($6\,^2P_{3/2}\rightarrow6\,^2S_{1/2}$), the excited state is composed of the hyperfine states. Therefore, the polarization state is mixed even for a well-defined TE or TM excitation. Based on the agreement between our quantum and classical treatments, it is straightforward to evaluate experimental results by taking all the hyperfine components into account and averaging over the atomic distance Z from the surface, accounting for the Cs vapor experiment [12]. As shown already in our previous work with the semiclassical evaluation, the theoretical results reproduce the experimental results very well.

VIII. CONCLUSION

We have developed a second-quantization formalism of electromagnetic fields including evanescent waves based on the detector-mode functions defined as the time reversal and spatial rotation of the triplet-mode functions. This provides a convenient basis for the evaluation of atomic and molecular radiation near a dielectric boundary surface, especially for a practical setup, in which a single photodetector is assumed in the far-field region. The detector-mode formalism provides us with a clear understanding of quantum radiation processes

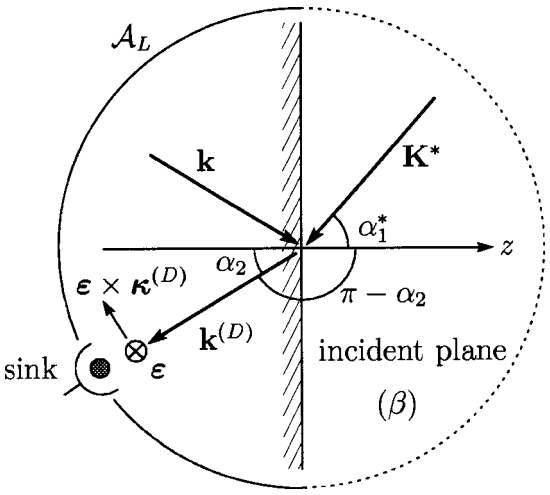

FIG. 5. The incident and refracted angles and polarization vectors. The incident plane makes an angle of β to the zx plane.

in terms of their classical correspondence. In fact, we have considered the radiation from an atom placed near a planar dielectric surface and found that the two components $\mathcal{E}_{DR}^{(I)}$ and $\mathcal{E}_{DR}^{(R)}$ of the R detector mode $\mathcal{E}_{DR}$ can be related, respectively, to the radiation fields from a real dipole and an image dipole in entirely free space, involving an outgoing wave to be coupled with a single photodetector placed in the vacuum-side far field. On the other hand, the component $\mathcal{E}_{DL}^{(T)}$ of the L detector mode $\mathcal{E}_{DL}$ represents the radiation field involving an outgoing wave from an electric dipole in an entirely filled medium, into a single photodetector placed in the medium-side far field. Such a direct comparison of quantum radiation processes with semiclassical ones makes it easy to evaluate the electromagnetic final-state density. This point is essential for studies of the atomic radiative lifetime and its modulation due to variations in the electromagnetic environment. A study of the interaction of atoms with the L detector mode would be one of the most interesting issues with respect to optical near-field phenomena and cavity-quantum-electrodynamics problems, since the L detector mode includes evanescent waves. With respect to coherent interaction processes such as multiple scattering of radiation and associated level shifts, both the detector-mode and triplet-mode formalisms provide us with a convenient basis for theoretical consideration. As an extension of the present work, we have derived a general analytic expression for the angular distribution of radiation from electric and magnetic multipoles near a planar dielectric surface by using the transformations of detector-mode functions into vector spherical-mode functions reported in our previous paper [21]. Further, based on the formalisms provided in the present work, we have evaluated modulations of the radiative lifetimes of electric and magnetic multipoles of arbitrary order due to near-field interactions at a boundary surface. These results will be published elsewhere. These results should be useful not only in basic cavity-QED studies but also in theoretical studies of optical near-field diagnosis and control of quantum electronic systems in a wide variety of mesoscopic devices, such as quantum dots and wires. It is especially important to give careful consideration of observation processes and associated signal transport properties in systems showing quantum-mechanical properties. The detector modes, coupled with multipole expansions and mode transforms by means of the angular spectrum representation, would serve as a convenient basis for these theoretical studies.

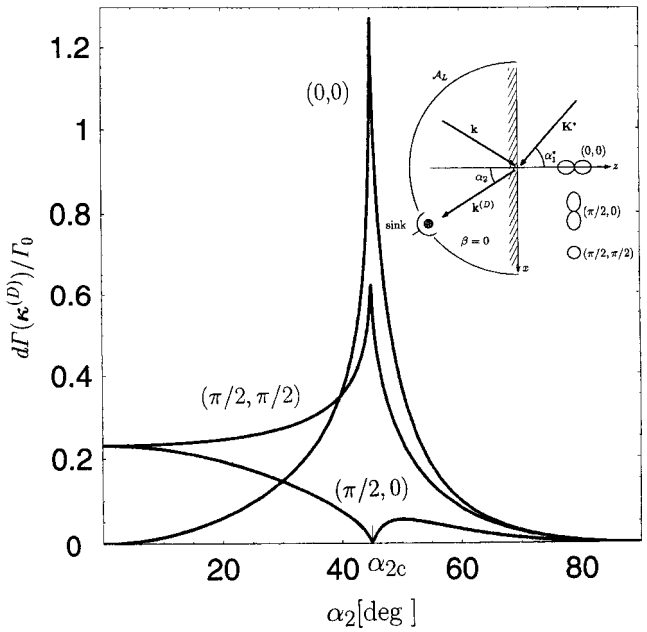

FIG. 6. The numerical results for the normalized differential emission rate, which is equivalent to the angular intensity distribution from an electric dipole oriented to $(\Theta,\Phi)=(0,0)$, $(\pi/2, 0)$, and $(\pi/2, \pi/2)$. The light emission is observed at a point on the intersection of the hemisphere $\mathcal{A}_L$ and the zx plane. α_{2c} is the critical angle of total internal reflection. Numerical results are given for $n=\sqrt{2}$ $(\alpha_{2c}=\pi/4)$, $\rho=1$.

ACKNOWLEDGMENTS

The authors would like to express their thanks to Professor I. Banno and Professor K. Kitahara for useful discussions and comments. This work was supported partly by a Grant in Aid for Scientific Research by the Ministry of Education, Science, Sports and Culture. The authors also thank the Matsuo Foundation for support.

APPENDIX A: TRIPLET-MODE FUNCTIONS

Here, in order to make notations of triplet modes clear and being coincident with the detector-mode formalisms in the present work, we will define the wave components of L- and R-triplet-mode functions.

1. Triplet-mode functions

Following Carniglia and Mandel [18], the L triplet mode functions [see Fig. 1(a)] are defined with respect to the electric field as a composition of incident, reflected, and transmitted fields by

$$\boldsymbol{\mathcal{E}}_L(\mathbf{k},\mu,\mathbf{r})=\boldsymbol{\mathcal{E}}_L^{(I)}(\mathbf{k},\mu,\mathbf{r})+\boldsymbol{\mathcal{E}}_L^{(R)}(\mathbf{k}^{(D)},\mu,\mathbf{r})+\boldsymbol{\mathcal{E}}_L^{(T)}(\mathbf{K}^{(D)},\mu,\mathbf{r}). \tag{A1}$$

Here, the subscript L indicates light incident from the medium side (left to the planar boundary). The components of L triplet-mode functions for TE and TM polarizations are written explicitly, using our definition of incoming wave vectors $\mathbf{k}$ and $\mathbf{K}$ and outgoing wave vectors $\mathbf{k}^{(D)}$ and $\mathbf{K}^{(D)}$ (see Sec. II), as follows:

$$\boldsymbol{\mathcal{E}}_L^{(I)}(\mathbf{k},1,\mathbf{r})=\begin{cases}\dfrac{1}{\sqrt{2}n}\boldsymbol{\varepsilon}\exp(i\mathbf{k}\cdot\mathbf{r}) & \text{for } z<0\\ \mathbf{0} & \text{for } z\geqslant 0,\end{cases} \tag{A2}$$

$$\boldsymbol{\mathcal{E}}_L^{(R)}(\mathbf{k}^{(D)},1,\mathbf{r})=\begin{cases}\dfrac{1}{\sqrt{2}n}\boldsymbol{\varepsilon}\dfrac{k_z+K_z}{k_z-K_z}\exp(i\mathbf{k}^{(D)}\cdot\mathbf{r}) & \text{for } z<0\\ \mathbf{0} & \text{for } z\geqslant 0,\end{cases} \tag{A3}$$

$$\boldsymbol{\mathcal{E}}_L^{(T)}(\mathbf{K}^{(D)},1,\mathbf{r})=\begin{cases}\dfrac{1}{\sqrt{2}n}\boldsymbol{\varepsilon}\dfrac{2k_z}{k_z-K_z}\exp(i\mathbf{K}^{(D)}\cdot\mathbf{r}) & \text{for } z\geqslant 0\\ \mathbf{0} & \text{for } z<0,\end{cases} \tag{A4}$$

$$\boldsymbol{\mathcal{E}}_L^{(I)}(\mathbf{k},2,\mathbf{r})=\begin{cases}-\dfrac{1}{\sqrt{2}n}(\boldsymbol{\kappa}\times\boldsymbol{\varepsilon})\exp(i\mathbf{k}\cdot\mathbf{r}) & \text{for } z<0\\ \mathbf{0} & \text{for } z\geqslant 0,\end{cases} \tag{A5}$$

$$\boldsymbol{\mathcal{E}}_L^{(R)}(\mathbf{k}^{(D)},2,\mathbf{r})=\begin{cases}-\dfrac{1}{\sqrt{2}n}(\boldsymbol{\kappa}^{(D)}\times\boldsymbol{\varepsilon})\dfrac{k_z+n^2K_z}{k_z-n^2K_z}\exp(i\mathbf{k}^{(D)}\cdot\mathbf{r}) & \text{for } z<0\\ \mathbf{0} & \text{for } z\geqslant 0,\end{cases} \tag{A6}$$

$$\boldsymbol{\mathcal{E}}_L^{(T)}(\mathbf{K}^{(D)},2,\mathbf{r})=\begin{cases}-\dfrac{1}{\sqrt{2}n}(\mathbf{c}^{(D)}\times\boldsymbol{\varepsilon})\dfrac{2nk_z}{k_z-n^2K_z}\exp(i\mathbf{K}^{(D)}\cdot\mathbf{r}) & \text{for } z\geqslant 0\\ \mathbf{0} & \text{for } z<0,\end{cases} \tag{A7}$$

where $\boldsymbol{\varepsilon}=\boldsymbol{\varepsilon}(\mathbf{k}_\parallel)$ is a real unit vector orthogonal to the wave vectors lying on the boundary plane $z=0$, so that $\boldsymbol{\varepsilon}$ indicates the polarization vector of TE waves. $\boldsymbol{\kappa}$, $\boldsymbol{\kappa}^{(D)}$, and $\mathbf{c}^{(D)}$ are unit vectors directing, respectively, $\mathbf{k}$, $\mathbf{k}^{(D)}$, and $\mathbf{K}^{(D)}$. Since a light source is assumed to be placed on $\mathcal{A}_L$ as shown in Fig. 1(a), we consider $\boldsymbol{\mathcal{E}}_L^{(I)}(\mathbf{k},\mu,\mathbf{r})$ as homogeneous waves, so that $\mathbf{k}$ is a real vector with components

$$-\infty<k_x<+\infty,\quad -\infty<k_y<+\infty,\quad 0<k_z<+\infty.$$

The corresponding wave-vector component K_z on the other side of the boundary is a real number for $0\leqslant k_x^2+k_y^2<K^2$, but a complex number for $K^2\leqslant k_x^2+k_y^2<n^2K^2$. Therefore, $\boldsymbol{\kappa}$ and $\boldsymbol{\kappa}^{(D)}$ always form real vectors, but $\mathbf{c}^{(D)}$ possibly involves a complex component.

The R triplet-mode functions [see Fig. 1(b)] are also defined by

$$\boldsymbol{\mathcal{E}}_R(\mathbf{K},\mu,\mathbf{r})=\boldsymbol{\mathcal{E}}_R^{(I)}(\mathbf{K},\mu,\mathbf{r})+\boldsymbol{\mathcal{E}}_R^{(R)}(\mathbf{K}^{(D)},\mu,\mathbf{r})+\boldsymbol{\mathcal{E}}_R^{(T)}(\mathbf{k}^{(D)},\mu,\mathbf{r}). \tag{A8}$$

Here, the suffix R indicates light incident from the vacuum side (right to the boundary). The three components of the R triplet-mode functions for TE and TM polarizations are written explicitly as follows:

$$\boldsymbol{\mathcal{E}}_R^{(I)}(\mathbf{K},1,\mathbf{r})=\begin{cases}\dfrac{1}{\sqrt{2}}\boldsymbol{\varepsilon}\exp(i\mathbf{K}\cdot\mathbf{r}) & \text{for } z\geqslant 0\\ \mathbf{0} & \text{for } z<0,\end{cases} \tag{A9}$$

$$\boldsymbol{\mathcal{E}}_R^{(R)}(\mathbf{K}^{(D)},1,\mathbf{r})=\begin{cases}\dfrac{1}{\sqrt{2}}\boldsymbol{\varepsilon}\dfrac{K_z+k_z}{K_z-k_z}\exp(i\mathbf{K}^{(D)}\cdot\mathbf{r}) & \text{for } z\geqslant 0\\ \mathbf{0} & \text{for } z<0,\end{cases} \tag{A10}$$

$$\boldsymbol{\mathcal{E}}_R^{(T)}(\mathbf{k}^{(D)},1,\mathbf{r})=\begin{cases}\dfrac{1}{\sqrt{2}}\boldsymbol{\varepsilon}\dfrac{2K_z}{K_z-k_z}\exp(i\mathbf{k}^{(D)}\cdot\mathbf{r}) & \text{for } z<0\\ \mathbf{0} & \text{for } z\geqslant 0,\end{cases} \tag{A11}$$

$$\boldsymbol{\mathcal{E}}_R^{(I)}(\mathbf{K},2,\mathbf{r})=\begin{cases}-\dfrac{1}{\sqrt{2}}(\mathbf{c}\times\boldsymbol{\varepsilon})\exp(i\mathbf{K}\cdot\mathbf{r}) & \text{for } z\geqslant 0\\ \mathbf{0} & \text{for } z<0,\end{cases} \tag{A12}$$

$$\boldsymbol{\mathcal{E}}_R^{(R)}(\mathbf{K}^{(D)},2,\mathbf{r})=\begin{cases}-\dfrac{1}{\sqrt{2}}(\mathbf{c}^{(D)}\times\boldsymbol{\varepsilon})\dfrac{n^2K_z+k_z}{n^2K_z-k_z}\exp(i\mathbf{K}^{(D)}\cdot\mathbf{r}) & \text{for } z\geqslant 0\\ \mathbf{0} & \text{for } z<0,\end{cases} \tag{A13}$$

$$\boldsymbol{\mathcal{E}}_R^{(T)}(\mathbf{k}^{(D)},2,\mathbf{r})=\begin{cases}-\dfrac{1}{\sqrt{2}}(\boldsymbol{\kappa}^{(D)}\times\boldsymbol{\varepsilon})\dfrac{2nK_z}{n^2K_z-k_z}\exp(i\mathbf{k}^{(D)}\cdot\mathbf{r}) & \text{for } z<0\\ \mathbf{0} & \text{for } z\geqslant 0,\end{cases} \tag{A14}$$

where $\mathbf{c}$ is the unit vector directing $\mathbf{K}$. Since the incident wave $\boldsymbol{\mathcal{E}}_R^{(I)}(\mathbf{K},\mu,\mathbf{r})$ is assumed to be coupled with a light source placed in the far-field region as shown in Fig. 1(b), we consider $\boldsymbol{\mathcal{E}}_R^{(I)}(\mathbf{K},\mu,\mathbf{r})$ as homogeneous waves with real wave vector $\mathbf{K}$ with components

$$-\infty<K_x<+\infty, \quad -\infty<K_y<+\infty, \quad -\infty<K_z<0.$$

The corresponding wave-vector component k_z on the other side of the boundary is a real number since $0\leqslant k_x^2+k_y^2=K_x^2+K_y^2<K^2$. Therefore, $\mathbf{c}^{(D)}$, $\mathbf{c}$, and $\boldsymbol{\kappa}^{(D)}$ always form real vectors.

According to the translational symmetry of the system along the x and y directions, L and R triplet modes correspond to eigenstates of the operator $-i\hbar\boldsymbol{\nabla}_{\parallel}=-i\hbar(\partial/\partial x,\partial/\partial y,0)$:

$$(-i\hbar\nabla_{\parallel})\boldsymbol{\mathcal{E}}_L(\mathbf{k},\mu,\mathbf{r})=(\hbar\mathbf{k}_{\parallel})\boldsymbol{\mathcal{E}}_L(\mathbf{k},\mu,\mathbf{r}), \tag{A15}$$

$$(-i\hbar\nabla_{\parallel})\boldsymbol{\mathcal{E}}_R(\mathbf{K},\mu,\mathbf{r})=(\hbar\mathbf{k}_{\parallel})\boldsymbol{\mathcal{E}}_R(\mathbf{K},\mu,\mathbf{r}). \tag{A16}$$

The orthogonality relations for L and R triplet mode functions [18] are given by

$$\int [\boldsymbol{\mathcal{E}}_L(\mathbf{k},\mu,\mathbf{r})]^*\cdot\boldsymbol{\mathcal{E}}_L(\mathbf{k}',\mu',\mathbf{r})n^2(\mathbf{r})d^3x = \frac{1}{2}(2\pi)^3\delta_{\mu,\mu'}\delta^3(\mathbf{k}-\mathbf{k}'), \tag{A17}$$

$$\int [\boldsymbol{\mathcal{E}}_R(\mathbf{K},\mu,\mathbf{r})]^*\cdot\boldsymbol{\mathcal{E}}_R(\mathbf{K}',\mu',\mathbf{r})n^2(\mathbf{r})d^3x = \frac{1}{2}(2\pi)^3\delta_{\mu,\mu'}\delta^3(\mathbf{K}-\mathbf{K}'), \tag{A18}$$

$$\int [\boldsymbol{\mathcal{E}}_L(\mathbf{k},\mu,\mathbf{r})]^*\cdot\boldsymbol{\mathcal{E}}_R(\mathbf{K}',\mu',\mathbf{r})n^2(\mathbf{r})d^3x=0. \tag{A19}$$

2. Field quantization based on triplet-mode functions

As a preparation, we will briefly review the field quantization based on the triplet modes [11] according to our description of the L and R modes. For planar boundary problems, an arbitrary electric field is expanded in terms of the triplet-mode functions as

$$\begin{aligned}\hat{\mathbf{E}}(\mathbf{r},t)=&\frac{1}{(2\pi)^{3/2}}\int_{k_z>0}d^3k\sum_{\mu=1}^{2}\left(\frac{\hbar K}{\epsilon}\right)^{1/2}\\&\times[\hat{a}_L(\mathbf{k},\mu)\mathcal{E}_L(\mathbf{k},\mu,\mathbf{r})e^{-iKt}+\text{c.c.}]\\&+\frac{1}{(2\pi)^{3/2}}\int_{K_z<0}d^3K\sum_{\mu=1}^{2}\left(\frac{\hbar K}{\varepsilon_0}\right)^{1/2}\\&\times[\hat{a}_R(\mathbf{K},\mu)\mathcal{E}_R(\mathbf{K},\mu,\mathbf{r})e^{-iKt}+\text{c.c.}],\end{aligned} \tag{A20}$$

with

$$\int_{k_z>0}d^3k=\int_{-\infty}^{\infty}\int_{-\infty}^{\infty}\int_{0}^{\infty}dk_xdk_ydk_z,$$

$$\int_{K_z<0}d^3K=\int_{-\infty}^{\infty}\int_{-\infty}^{\infty}\int_{-\infty}^{0}dK_xdK_ydK_z.$$

Here we have replaced $\hat{u}(\mathbf{k},\mu)$ and $\hat{v}(\mathbf{K},\mu)$ in Ref. [11], respectively, by $\hat{a}_L(\mathbf{k},\mu)=\hat{u}(\mathbf{k},\mu)/[(2\pi)^3\hbar]^{1/2}$ and $\hat{a}_R(\mathbf{K},\mu)=\hat{v}(\mathbf{K},\mu)/[(2\pi)^3\hbar]^{1/2}$. The quantization of electric field is achieved by considering the expansion coefficients $\hat{a}_L(\mathbf{k},\mu)$ and $\hat{a}_R(\mathbf{K},\mu)$ as quantum-mechanical operators and replacing the complex conjugate by the Hermitian conjugate. Here, $\hat{a}_L(\mathbf{k},\mu)$ and $\hat{a}_R(\mathbf{K},\mu)$ correspond to the annihilation operators for L and R triplet modes, respectively, which satisfy the following commutation relations:

$$[\hat{a}_L(\mathbf{k},\mu),\hat{a}_L^{\dagger}(\mathbf{k}',\mu')]=\delta_{\mu,\mu'}\delta(\mathbf{k}-\mathbf{k}'), \tag{A21}$$

$$[\hat{a}_R(\mathbf{K},\mu),\hat{a}_R^{\dagger}(\mathbf{K}',\mu')]=\delta_{\mu,\mu'}\delta(\mathbf{K}-\mathbf{K}'), \tag{A22}$$

$$[\hat{a}_R(\mathbf{K},\mu),\hat{a}_L(\mathbf{k}',\mu')]=0, \tag{A23}$$

$$[\hat{a}_R(\mathbf{K},\mu),\hat{a}_L^{\dagger}(\mathbf{k}',\mu')]=0. \tag{A24}$$

We can construct the Hamiltonian $\hat{\mathcal{H}}$, number operator $\hat{\mathcal{N}}$, and pseudomomentum operator $\hat{\boldsymbol{\mathcal{P}}}_{\parallel}$, according to the orthodox procedure of second quantization as follows:

$$\begin{aligned}\hat{\mathcal{H}}=&\int_{k_z>0}d^3k\sum_{\mu=1}^{2}\hbar K\hat{a}_L^{\dagger}(\mathbf{k},\mu)\hat{a}_L(\mathbf{k},\mu)\\&+\int_{K_z<0}d^3K\sum_{\mu=1}^{2}\hbar K\hat{a}_R^{\dagger}(\mathbf{K},\mu)\hat{a}_R(\mathbf{K},\mu),\end{aligned} \tag{A25}$$

$$\begin{aligned}\hat{\mathcal{N}}=&\int_{k_z>0}d^3k\sum_{\mu=1}^{2}\hat{a}_L^{\dagger}(\mathbf{k},\mu)\hat{a}_L(\mathbf{k},\mu)\\&+\int_{K_z<0}d^3K\sum_{\mu=1}^{2}\hat{a}_R^{\dagger}(\mathbf{K},\mu)\hat{a}_R(\mathbf{K},\mu),\end{aligned} \tag{A26}$$

$$\begin{aligned}\hat{\mathcal{P}}=&\int_{k_z>0}d^3k\sum_{\mu=1}^{2}\hbar\mathbf{k}_{\parallel}\hat{a}_L^{\dagger}(\mathbf{k},\mu)\hat{a}_L(\mathbf{k},\mu)\\&+\int_{K_z<0}d^3K\sum_{\mu=1}^{2}\hbar\mathbf{k}_{\parallel}\hat{a}_R^{\dagger}(\mathbf{K},\mu)\hat{a}_R(\mathbf{K},\mu).\end{aligned} \tag{A27}$$

The number eigenstates can be produced by operating $\hat{a}_L^{\dagger}(\mathbf{k},\mu)$ or $\hat{a}_R^{\dagger}(\mathbf{K},\mu)$ on the vacuum state $|0\rangle$ with the normalization $\langle 0|0\rangle=1$. For example, the single-photon states $(N=1)$ with energy $\hbar K$, pseudomomentum $\hbar\mathbf{k}_{\parallel}$, and polarization μ are given by

$$|T,1(\mathbf{k},\mu)\rangle=\hat{a}_L^{\dagger}(\mathbf{k},\mu)|0\rangle, \tag{A28}$$

$$|T,1(\mathbf{K},\mu)\rangle=\hat{a}_R^{\dagger}(\mathbf{K},\mu)|0\rangle, \tag{A29}$$

with the normalization relations

$$\langle T,1(\mathbf{k},\mu)|T,1(\mathbf{k}',\mu')\rangle=\delta_{\mu,\mu'}\delta(\mathbf{k}-\mathbf{k}'), \tag{A30}$$

$$\langle T,1(\mathbf{K},\mu)|T,1(\mathbf{K}',\mu')\rangle=\delta_{\mu,\mu'}\delta(\mathbf{K}-\mathbf{K}'), \tag{A31}$$

$$\langle T,1(\mathbf{k},\mu)|T,1(\mathbf{K}',\mu')\rangle=0, \tag{A32}$$

where the label T indicates photonic states corresponding to the triplet modes. It is noted again that the wave vectors $\mathbf{k}$ and $\mathbf{K}$ are used to specify those of the L and R modes, respectively.

APPENDIX B: TIME REVERSAL AND SPATIAL ROTATION

Here we study the behavior of the triplet-mode functions under the time-reversal transform and spatial rotation with angle π around the z axis.

1. Time-reversal (T) transform

The electromagnetic fields satisfy Maxwell's equations

$$\nabla\times\mathbf{E}(\mathbf{r},t)=-(\partial/\partial t)\mathbf{B}(\mathbf{r},t), \tag{B1}$$

$$\nabla\times\mathbf{B}(\mathbf{r},t)=n^2(\mathbf{r})(\partial/\partial t)\mathbf{E}(\mathbf{r},t). \tag{B2}$$

According to Eqs. (B1) and (B2), the Fourier components of the electromagnetic fields $\mathbf{E}_{(+)}(\mathbf{r},t)=\mathbf{E}(\mathbf{r})\exp(-iKt)$ and $\mathbf{B}_{(+)}(\mathbf{r},t)=\mathbf{B}(\mathbf{r})\exp(-iKt)$ for the light frequency K satisfy the equations

$$\nabla\times\mathbf{E}_{(+)}(\mathbf{r},t)=iK\mathbf{B}_{(+)}(\mathbf{r},t), \tag{B3}$$

$$\nabla\times\mathbf{B}_{(+)}(\mathbf{r},t)=-in^2(\mathbf{r})K\mathbf{E}_{(+)}(\mathbf{r},t). \tag{B4}$$

Under the time-reversal operation (T transform), the Fourier components of the electric and magnetic fields are transformed as

$$\mathbf{E}_{(+)}(\mathbf{r},t)\rightarrow[\mathbf{E}_{(+)}(\mathbf{r},-t)]^*, \tag{B5}$$

$$\mathbf{B}_{(+)}(\mathbf{r},t)\rightarrow-[\mathbf{B}_{(+)}(\mathbf{r},-t)]^*, \tag{B6}$$

where the asterisk denotes the complex conjugate. We will consider the behavior of L triplet-mode functions under the T transform, which is straightforward for the wave vectors of incident, reflected, and transmitted components:

$$\mathbf{k}\rightarrow-\mathbf{k},\quad \mathbf{k}^{(D)}\rightarrow-\mathbf{k}^{(D)},\quad \mathbf{K}^{(D)}\rightarrow-\mathbf{K}^{(D)*}.$$

When we consider an observation scheme to be coupled with the photonic system under consideration, a single light source is transformed into a single light sink. Since the sign in the z component of each wave vector is changed for real values of K_z, the time-reversal operator transforms the L triplet-mode functions into mode functions involving an outgoing wave to the left-hand side half space (medium) of the boundary. For imaginary values of K_z, the sign in the z components of $\mathbf{K}^{(D)}$ remains unchanged, and the transmitted component of the triplet presents a damped wave along the z direction.

Similarly, under the time-reversal operation, the wave vectors of incident, reflected, and transmitted components of the R triplet-mode functions are transformed as

$$\mathbf{K}\rightarrow-\mathbf{K},\quad \mathbf{K}^{(D)}\rightarrow-\mathbf{K}^{(D)},\quad \mathbf{k}^{(D)}\rightarrow-\mathbf{k}^{(D)}.$$

Thus the single light source assumed is transformed into a single light sink. Since the sign of the z component of each wave vector is changed, the time-reversal operation transforms the R triplet-mode functions into mode functions involving a single outgoing wave into the right-hand side half space (vacuum) of the boundary.

In addition, under the time-reversal operation, the sign of x and y components of every wave vector changes as $\hbar\mathbf{k}_{\|}\rightarrow-\hbar\mathbf{k}_{\|}$.

2. Spatial rotation (C_2) transformation

We consider next the behavior of electric and magnetic fields under the spatial rotation C_2 with angle π around the z axis (a two-dimensional inversion with respect to the incident plane). As we use $\mathbf{r}^{(D)}=(x,y,-z)$ for the transformed position vector corresponding to $\mathbf{r}=(x,y,z)$, the spatial rotation C_2 is given by the transform $\mathbf{r}\rightarrow-\mathbf{r}^{(D)}$. Under the transform C_2, the refractive-index function is unchanged as $n(\mathbf{r})\rightarrow n(-\mathbf{r}^{(D)})=n(\mathbf{r})$. Therefore, the Fourier components of electric and magnetic fields are transformed as

$$\mathbf{E}_{(+)}(\mathbf{r},t)\rightarrow-\mathbf{E}^{(D)}_{(+)}(-\mathbf{r}^{(D)},t), \tag{B7}$$

$$\mathbf{B}_{(+)}(\mathbf{r},t)\rightarrow-\mathbf{B}^{(D)}_{(+)}(-\mathbf{r}^{(D)},t), \tag{B8}$$

where $\mathbf{E}_{(+)}=(E_x,E_y,E_z)$, $\mathbf{B}_{(+)}=(B_x,B_y,B_z)$, $\mathbf{E}^{(D)}_{(+)}=(E_x,E_y,-E_z)$, and $\mathbf{B}^{(D)}_{(+)}=(B_x,B_y,-B_z)$, according to our usage of the label (D).

Under C_2, the incident, reflected, and transmitted wave vectors in L and R triplet-mode functions are transformed as

$$\mathbf{k}\rightarrow-\mathbf{k}^{(D)},\quad \mathbf{k}^{(D)}\rightarrow-\mathbf{k},\quad \mathbf{K}^{(D)}\rightarrow-\mathbf{K},$$

$$\mathbf{K}\rightarrow-\mathbf{K}^{(D)},\quad \mathbf{K}^{(D)}\rightarrow-\mathbf{K},\quad \mathbf{k}^{(D)}\rightarrow-\mathbf{k}.$$

When we consider an observation process, the position of the light source is rotated by the angle π around the z axis. In addition, C_2 transforms the pseudomomentum as $\hbar\mathbf{k}_{\|}\rightarrow-\hbar\mathbf{k}_{\|}$.

[1] *Cavity Quantum Electrodynamics*, edited by P. Berman (Academic, San Diego, 1994).

[2] C. J. Hood, M. S. Chapman, T. W. Lynn, and H. J. Kimble, Phys. Rev. Lett. **80**, 4157 (1998).

[3] G. S. Agarwal, Phys. Rev. A **11**, 230 (1975); **11**, 243 (1975); **11**, 253 (1975).

[4] J. M. Wylie and J. E. Sipe, Phys. Rev. A **30**, 1185 (1984).

[5] See, for example, articles in *Near Field Optics*, edited by D. W. Pohl and D. Courjon (Kluwer, Dordrecht, 1993).

[6] M. Ohtsu and H. Hori, *Near-Field Nano-Optics* (Academic/Plenum, New York, 1999), p. 300.

[7] S. D. Gupta and G. S. Agarwal, Opt. Commun. **115**, 597 (1995).

[8] H. Chew, Phys. Rev. A **38**, 3410 (1988).

[9] J. Ye, D. W. Vernooy, and H. J. Kimble, Phys. Rev. Lett. **83**, 4987 (1999).
[10] D. W. Vernooy, A. Furusawa, N. Ph. Georgiades, V. S. Ilchenko, and H. J. Kimble, Phys. Rev. A **57**, R2293 (1998).
[11] C. K. Carniglia, L. Mandel, and K. H. Drexhage, J. Opt. Soc. Am. **62**, 479 (1972).
[12] T. Matsudo, T. Inoue, Y. Inoue, H. Hori, and T. Sakurai, Phys. Rev. A **55**, 2406 (1997).
[13] T. Matsudo, Y. Takahara, H. Hori, and T. Sakurai, Opt. Commun. **145**, 64 (1998).
[14] C. G. Aminoff, A. M. Steane, P. Bouyer, P. Desbiolles, J. Dalibard, and C. Cohen-Tannoudji, Phys. Rev. Lett. **71**, 3083 (1993).
[15] H. Ito, T. Nakata, K. Sakaki, M. Otsu, K. I. Lee, and W. Jhe, Phys. Rev. Lett. **76**, 4500 (1996).
[16] V. I. Balykin, V. S. Letokhov, Yu. B. Ovchinnikov, and A. I. Sidorov, Phys. Rev. Lett. **60**, 2137 (1988).
[17] M. Born and E. Wolf, *Principles of Optics* 6th ed. (Pergamon, Oxford, 1980), p. 563.
[18] C. K. Carniglia and L. Mandel, Phys. Rev. D **3**, 280 (1971).
[19] J. M. Vigoureux and R. Payen, J. Phys. (France) **36**, 1327 (1975).
[20] E. Wolf and M. Nieto-Vesperinas, J. Opt. Soc. Am. A **2**, 886 (1985).
[21] T. Inoue, I. Banno, and H. Hori, Opt. Rev. **5**, 295 (1998).
[22] T. Inoue and H. Hori, Opt. Rev. **3**, 458 (1996).
[23] W. Lukosz and R. E. Kunz, J. Opt. Soc. Am. **67**, 1607 (1977).
[24] W. Lukosz and R. E. Kunz, J. Opt. Soc. Am. **67**, 1615 (1977).
[25] W. Lukosz, J. Opt. Soc. Am. **69**, 1495 (1979).
[26] T. Saiki, K. Nishi, and M. Ohtsu, Jpn. J. Appl. Phys., Part 1 **37**, 1638 (1998).
[27] W. Jhe and K. Jang, Phys. Rev. A **53**, 1126 (1996).
[28] V. V. Klimov and V. S. Letokhov, Opt. Commun. **122**, 155 (1996).
[29] T. Inoue and H. Hori (unpublished).